



Published in final edited form as:

J Lab Autom. 2015 April ; 20(2): 107–126. doi:10.1177/2211068214561025.

TEER measurement techniques for *in vitro* barrier model systems

Balaji Srinivasan¹, Aditya Reddy Kolli¹, Mandy Brigitte Esch², Hasan Erbil Abaci², Michael L. Shuler^{2, **}, and James J. Hickman^{1,3, **}

¹NanoScience Technology Center, University of Central Florida

²Biomedical Engineering, Cornell University, USA

³Biomolecular Science Center, Burnett School of Biomedical Sciences, University of Central Florida, USA

Abstract

Transepithelial/transendothelial electrical resistance (TEER) is a widely accepted quantitative technique to measure the integrity of tight junction dynamics in cell culture models of endothelial and epithelial monolayers. TEER values are strong indicators of the integrity of the cellular barriers before they are evaluated for transport of drugs or chemicals. TEER measurements can be performed in real-time without cell damage and generally are based on measuring ohmic resistance or measuring impedance across a wide spectrum of frequencies. TEER measurements for various cell types have been reported with commercially available measurement systems and also with custom built microfluidic implementations. Some of the barrier models that have been widely characterized utilizing TEER include the blood-brain barrier (BBB), gastrointestinal (GI) tract, and pulmonary models. Variations in TEER value can arise due to factors such as temperature, medium formulation and passage number of cells. The aim of this paper is to review the different TEER measurement techniques and analyze their strengths and weaknesses, the significance of TEER in drug toxicity studies, examine the various *in vitro* models and microfluidic organs-on-chips implementations utilizing TEER measurements in some widely studied barrier models (BBB, GI tract and pulmonary), and discuss the various factors that can affect TEER measurements.

Keywords

TEER; Impedance Spectroscopy; organs-on-chips; *in vitro* barrier models; drug toxicity

1. Introduction

Endothelial cells provide a nonthrombogenic monolayer surface that lines the lumen of blood vessels and functions as a cellular interface between blood and tissue.¹ Epithelial cells

**Corresponding Authors: James J Hickman, University of Central Florida, NanoScience Technology Center, 12424 Research, Parkway, Suite 400, Orlando, FL 32826, Phone: 407-823-1925, Fax: 407-882-2819, jhickman@mail.ucf.edu; Michael L. Shuler, Cornell University, Department of Biomedical Engineering, 115 Weill Hall Cornell University, Ithaca, NY 14853, Phone: 607-255-7577, Fax: 607-255-7330, mls50@cornell.edu.

line and provide a protective layer for both the outside and the inside cavities and lumen of the body.² Epithelial and endothelial cells are connected to each other via intercellular junctions that differ in their morphological appearance, composition and function. The tight junction or zona occludens is the intercellular junction that regulates diffusion³ and allows both of these cell layers to form selectively permeable cellular barriers that separate apical (luminal) and basolateral (abluminal) sides in the body, thereby controlling the transport processes to maintain homeostasis. Barrier integrity is vital for the physiological activities of the tissue. To successfully treat certain diseases of organs protected by physiological barriers, it is necessary to develop methods that can enable the transport of therapeutic drugs across these barriers in order to reach the target tissue.

Organs-on-chips⁴ or body-on-a-chip⁵⁻⁹ systems are microengineered biomimetic devices containing microfluidic channels and chambers populated by living cells, which replicate key functional units of living organs to reconstitute integrated organ-level pathophysiology *in vitro*. In recent years, organs-on-chips have garnered increasing attention due to both ethical and scientific reasons. In the European Union, *in vitro* methods will play a major role¹⁰ in future legislation on testing chemicals and also in relation to the seventh amendment to the *Cosmetic Directive*. Both of these policies call for broad replacement, reduction and refinement of animal experiments. Therefore, an extensive interest has been shown by many pharmaceutical, food and cosmetic industries in applying these body-on-a-chip systems for studying drug, nutrient and xenobiotic absorption and possible toxic effects.

The development of chip-based systems with *in vitro* cell barrier models can be used to study parameters that control permeability and predict drug transport across these barriers in the early stages of drug discovery. The growing interest in body-on-a-chip systems is due to their potential for providing a high throughput, cost-effective and reliable method for predicting drug interactions in humans including transport phenomena. These cell culture models also have an advantage of precisely controlling important transport parameters and experimental conditions. To perform permeability assessments on the cellular barriers, the complexity¹¹ of the *in vitro* models in these systems should reflect the variety of membrane transport systems, metabolic pathways involved and include a polarized cell layer. The *in vitro* models should also incorporate apical as well as basolateral compartments with appropriate composition of the aqueous medium on each side of the cell membrane. It may not be possible to develop a single *in vitro* system that can simulate all the *in vivo* conditions, but use of various *in vitro* systems with more than one type of cell (co-culture) as decision making tools in early drug discovery¹² is a common practice.

Numerous barrier systems¹³⁻¹⁴ for predicting drug permeability, typically including cell cultures grown on permeable membranes, have been reported. The configuration in these systems is designed to allow access to both apical and basolateral compartments. These models primarily include cells that grow in a monolayer when seeded on permeable membranes, and have physiologic characteristics similar to the barrier physiology and functionality. The successful application of a system to predict drug absorption depends on how closely the *in vitro* model can mimic the characteristics of the *in vivo* barrier integrity. These *in vitro* models can be based on primary cells¹⁵ or cell lines.¹⁶

To perform reliable *in vitro* experiments, qualitative and quantitative techniques have been developed to first confirm and quantify the barrier integrity before proceeding with drug testing. A freeze-fracture electron microscopy of transmembrane fibrils and immunostaining for proteins characteristic of tight junctions (occluding, ZO-1 and ZO-2) can provide qualitative insights into the barrier integrity of an endothelial or epithelial monolayer. A simple assay that has been widely used is based on the permeability of the barrier to paracellular tracer compounds of various molecular weights. The first use of sucrose (molecular weight: 342 Da) labeled with carbon-14 for flux measurement on a brain endothelial monolayer has been reported.¹⁷ Radiolabeled markers provide the required sensitivity, but they need special safety precautions for handling and storage. Radiolabeled markers have a short half-life and are not suitable for long term storage. Some of the other frequently used paracellular tracers include inulin (molecular weight: 5 kDa) and mannitol (molecular weight: 182 Da). Albumin (molecular weight: 67 kDa) is another transendothelial permeability marker and has been observed in endothelial vesicles.¹⁸ Evans blue dye–albumin complex,¹⁹ albumin,²⁰ or biotin–albumin²¹ are used for quantification of serum protein permeability. An alternative approach that has been used is based on non-radioactive fluorescence labeled marker proteins such as fluorescein isothiocyanate (FITC)-labeled dextrans.²² However, solutes labeled with nonradioactive fluorophore compounds do not provide the required sensitivity to reflect the subtle changes in monolayer permeability that are due to poor specific activity (fluorescence/mg protein) or fluorophore instability.²³ Enzymatic markers such as horseradish peroxidase (HRP) have also been used to study macromolecule diffusion across endothelial monolayers by tracking supernatant HRP activity.²³ However, the activity of the enzymatic markers can be affected by factors such as pH, temperature and serum constituents, thereby limiting their application. The permeability with these above methods is quantified by the endothelial permeability coefficient²⁴⁻²⁵ which is calculated based on the measured flux of the selected tracer across monolayers and cell-free inserts.

The use of tracer compounds can interfere with the transport process under study and can also affect the barrier integrity. Also, the use of chemical dyes renders the tested cells unusable for further experiments. Therefore, non-invasive techniques are best suited to continuously monitor the barrier integrity. Transepithelial/transendothelial electrical resistance (TEER) is the measurement of electrical resistance across a cellular monolayer and is a very sensitive and reliable method to confirm the integrity and permeability of the monolayer. Although the measurement of TEER and of trans-epithelial passage of marker molecules are both indicators of the integrity of the tight junctions and of the cell monolayer, they determine different experimental parameters.¹⁰ TEER reflects the ionic conductance of the paracellular pathway in the epithelial monolayer, whereas the flux of non-electrolyte tracers (expressed as permeability coefficient) indicates the paracellular water flow, as well as the pore size of the tight junctions.¹⁰ The advantages and wide use of the TEER method is because it is non-invasive and can be applied to monitor live cells during their various stages of growth and differentiation. This paper discusses some of the theoretical aspects of different TEER measurement techniques, examples of commercially available TEER measurement systems and their applications, a survey of TEER

measurement for *in vitro* models and microfluidic implementations of a few widely studied cellular barriers, and various factors that affect TEER measurements.

2. TEER Measurement Methods

2.1 Ohm's Law Method

The electrical resistance of a cellular monolayer, measured in ohms, is a quantitative measure of the barrier integrity.²⁶ The classical setup for measurement of TEER, as shown in Figure 1, consists of a cellular monolayer cultured on a semipermeable filter insert which defines a partition for apical (or upper) and basolateral (or lower) compartments. For electrical measurements, two electrodes are used, with one electrode placed in the upper compartment and the other in the lower compartment and the electrodes are separated by the cellular monolayer. In theory, the ohmic resistance can be determined by applying a direct current (DC) voltage to the electrodes and measuring the resulting current. The ohmic resistance is calculated based on Ohm's law as the ratio of the voltage and current. However, DC currents can damage both the cells and the electrodes. To overcome this issue, an alternating current (AC) voltage signal with a square waveform is applied. In the widely used and commercially available TEER measurement system known as an Epithelial Voltohmmeter (EVOM),²⁷ an AC square wave at a frequency of 12.5 Hz is used to avoid any charging effects on the electrodes and the cell layer. The EVOM system has a measurement range of 1-9,999 Ω with a 1 Ω resolution and uses a pair of electrodes popularly known as a STX2/"chopstick" electrode pair. Each stick of the electrode pair (4 mm wide and 1 mm thick) contains a silver/silver chloride pellet for measuring voltage and a silver electrode for passing current. The measurement procedure includes measuring the blank resistance (R_{BLANK}) of the semipermeable membrane only (without cells) and measuring the resistance across the cell layer on the semipermeable membrane (R_{TOTAL}). The cell specific resistance (R_{TISSUE}) in units of Ω , can be obtained as:

$$R_{TISSUE}(\Omega) = R_{TOTAL} - R_{BLANK}$$

Where resistance is inversely proportional²⁸ to the effective area of the semipermeable membrane (M_{AREA}) which is reported in units of cm^2 .

$$R_{TISSUE}(\Omega) \propto \frac{1}{M_{AREA}(cm^2)}$$

TEER values are typically²⁸⁻²⁹ reported ($TEER_{REPORTED}$) in units of $\Omega \cdot cm^2$ and calculated as:

$$TEER_{REPORTED} = R_{TISSUE}(\Omega) \times M_{AREA}(cm^2)$$

The TEER readings with EVOM2 are highly dependent on the electrode positions and a careful handling of the electrodes is required while introducing them into the well under test to avoid any disturbance to the cells. The uniformity of the current density generated by the electrodes across the cell layer has a significant effect on the TEER measurements. The STX2/chopstick electrode cannot deliver a uniform current density over a relatively large membrane,²⁷ such as the ones used in 24 mm diameter tissue culture inserts, and leads to an overestimation of the TEER value. As an alternative to STX2/chopstick electrodes, an EndOhm chamber³⁰ which allows the cups from culture wells to be inserted can be used. In an EndOhm chamber, both the chamber and the cap contain a pair of concentric electrodes: a voltage-sensing silver/silver chloride pellet in the center plus an annular current electrode. The symmetrical arrangement of circular disc electrodes on both sides of the membrane in an EndOhm chamber generates a more uniform current density across the membrane when compared to STX2/chopstick electrodes. Also, with Endohm's fixed electrode geometry, variation of measurements on a given sample is reduced³⁰ to 1-2 Ω when compared to 10-30 Ω with STX2 electrodes. Apart from the EVOM/STX2/EndOhm systems, a few of the other commercial systems available for TEER measurements include Electric Cell-Substrate Impedance Sensing (ECIS)³¹ (Applied BioPhysics Inc., Troy, NY), REMS AutoSampler (World Precision Instruments, Sarasota, FL), Millicell-ERS system^{10, 32} (Millipore Corp., Bedford, USA) and Ussing Chamber Systems³³ (Warner Instruments, Hamden, CT).

2.2 Impedance Spectroscopy

Impedance spectroscopy when combined with a fitting algorithm provides a more accurate representation of TEER values than traditional DC/single frequency AC measurement systems.³⁴ Impedance spectroscopy is performed by applying a small amplitude AC excitation signal with a frequency sweep and measuring the amplitude and phase response of the resulting current. Figure 2 (a) indicates a schematic which illustrates the concept of impedance measurement.

Electrical impedance (Z) is the ratio of the voltage-time function $V(t)$ and the resulting current-time function $I(t)$:

$$Z = \frac{V(t)}{I(t)} = \frac{V_o \sin \theta}{I_o \sin(2\pi ft + \Phi)} = \frac{1}{Y}$$

$$Z = Z_R + jZ_I$$

where V_o and I_o are the peak voltage and current, f is the frequency, t is the time, Φ is the phase shift between the voltage-time and current-time functions, and Y is the complex conductance or admittance. Z is a complex function and can be described by the modulus $|Z|$ and the phase shift Φ or by the real part Z_R and the imaginary part Z_I , as illustrated in the Figure 2(b). An in depth analysis of impedance spectroscopy has been published.³⁵

Impedance measurement across a wide spectrum of frequencies instead of a DC/single frequency AC TEER measurement can provide additional information about the capacitance of the cell layer. An automated measurement system (cellZscope[®], nanoAnalytics GmbH, Germany) has been developed for measuring the transendothelial/epithelial impedance of various barrier-forming cells cultured on permeable membranes of standard cell culture inserts. An equivalent circuit analysis of the measured impedance spectrum is performed to obtain the electrical parameters that can be applied to characterize the cellular barrier properties. Figure 3 (a) (adapted from Benson et al.²⁶) shows a typical equivalent circuit diagram that can be applied to analyze the impedance spectrum of cellular systems.²⁶ In this circuit, the current can flow through the junctions between cells (paracellular route) or through the cell membrane of the cells (transcellular route). The tight junction proteins in the paracellular route contribute to an ohmic resistance (R_{TEER}) in the equivalent circuit. Each lipid bilayer in the transcellular route contributes to a parallel circuit²⁶ consisting of ohmic resistance ($R_{membrane}$) and an electrical capacitance (C_C). In addition to these elements, the resistance of the cell culture medium (R_{medium}) and the capacitance of the measurement electrodes (C_E) also have to be considered. The high values of $R_{membrane}$ causes the current to mostly flow across the capacitor and allows an approximation where $R_{membrane}$ can be ignored²⁶ and the lipid bilayers can be represented with just C_C . Based on this approximation, the equivalent circuit diagram can be further simplified as shown in Figure 3 (b) (adapted from Benson et al.²⁶) and the impedance spectrum observed will have a non-linear frequency dependency as shown in Figure 3 (c) (adapted from Benson et al.²⁶). Typically, there are three distinct frequency regions in the impedance spectrum where the impedance is dominated by certain equivalent circuit elements. In the low frequency range, the impedance signal is dominated by C_E . In the mid frequency range, the impedance signal is dominated by circuit elements related to the cells, namely R_{TEER} and C_C . In the high frequency range, C_C and C_E provide a more conductive path and the impedance signal is dominated by R_{medium} . These equivalent circuit parameters can be estimated by fitting the experimental impedance spectrum data to the equivalent circuit model using non-linear least squares fitting techniques to obtain the best fit parameters.

The following sections describe the advantages of organs-on-chips for TEER measurement, *in vitro* models of some widely studied cellular barriers, TEER measurements with *in vitro* models and some microfluidic implementations, and the various factors affecting TEER values.

3. Organs-on-chips

The existing commercial systems for measuring TEER are mostly confined to static and macroscopic cellular environments. The STX/chopstick electrodes are not suitable for integration with body-on-a-chip systems due to the small cell culture area that is not easily accessible to allow electrode placement close to the cell culture area and variation between measurements when electrodes are not firmly secured in the same position. An integration of immobilized TEER electrodes directly within the chip model and in close proximity to the cellular monolayer can not only reduce the contribution of electrical resistance from the cell culture medium but also the signal noise generated by any electrode motion. The size of the electrodes can be scaled relative to the microchannel dimensions within the system. TEER

measurements can be achieved with much smaller surface areas in a chip-based system when compared to conventional culture systems. However, with custom designed and embedded TEER electrodes, it is important to ensure that a uniform current density across the cellular monolayer is achieved during measurement. The non-uniformity of current density has proved to be one of the reasons for erratic TEER values.³⁶ The electrode design process for these chips can be combined with electrical simulation/modeling to ensure that a uniform current density is achieved. Organs-on-chips also provide the advantage of enabling the study of cells under physiologically relevant fluid flow conditions that are known to induce mechanotransductive effect on certain cell types. For example, many transport processes in kidney are known to be regulated by fluid flow and shear stress.³⁷ *In vitro* chips also provide precise control over physiologic stresses,³⁸ chemical signaling³⁹ and degree of cell to cell interaction⁴⁰ while reducing reagent consumption.

4. Blood-Brain Barrier Model

The blood-brain barrier (BBB)⁴¹ is an active interface between the circulatory system and the central nervous system (CNS) which restricts the free movement of different substances between the two compartments and plays a crucial role in maintaining homeostasis in the CNS. Figure 4 (adapted from Wong et al.⁴²) shows a schematic of the various components of a BBB model. Physiologically, the BBB⁴³ consists of an intricate network of vascular endothelial cells which are quite distinct from other endothelium due to the combination of a physical and biochemical barrier. The BBB endothelial cells are surrounded by basal lamina and astrocytic perivascular end-feet with astrocytes providing the cellular link to the neurons. The BBB endothelium⁴³ is characterized by the presence of tight junctions, a lack of fenestrations and minimal pinocytotic vesicles. The tight junction consists of transmembrane proteins (claudin, occludin, and junction adhesion molecules) and cytoplasmic accessory proteins. The details of the principal components of the BBB and their functions have been previously published.^{41, 43-44} The BBB has a dual function of a carrier and a barrier. The barrier function of the BBB is to restrict transport of potentially toxic or harmful substances from the blood to the brain. The carrier function allows for selective transport of nutrients to the brain and removal of metabolites from the cerebral spinal fluid that surrounds CNS tissue. Small lipid soluble compounds (<500 Da) such as alcohol, narcotics and anticonvulsants can pass through the BBB with relative ease. However, the BBB inhibits⁴³ the brain from taking up 100% of large molecule therapeutics (> 1000 Da) that includes genes, recombinant proteins as well as more than 98% of potential neurotherapeutics comprised of proteins and peptides (500-1000 Da). The development of drugs that can cross the BBB is a challenge and consequently belies the importance of developing *in vitro* models of the BBB that can mimic *in vivo* barrier properties for evaluation of these drugs.

Establishing *in vitro* models of the BBB has been a challenging task due to species differences, low availability of human primary brain endothelial cells, and poor barrier formation by immortalized human brain microvascular endothelial cells. The primary cell cultures widely used are brain endothelial cells from a spectrum of mammals of rat, mouse, pig, bovine or human origin. Some of the well characterized brain endothelial cell lines⁴¹ includes RBE4 (rat origin), GP8 (rat origin) and hCMEC/D3 (human origin). Porcine⁴⁵ and

bovine⁴⁶ cell lines are also available but are not very well characterized. Although cerebral endothelial cells are the principal components of the BBB, there is increasing evidence of other cell types such as glial cells, pericytes and neurons playing important regulatory roles in the induction and maintenance of the BBB and can be included to develop more complex *in vitro* co-culture models of these systems.⁴⁷

TEER has been the most commonly used parameter to evaluate the functionality of the BBB since it was first introduced by Crone et al.⁴⁸ and was used to measure *in vivo* BBB properties of various species.⁴⁹⁻⁵⁰ Table 1 indicates a range of TEER values reported for BBB models. More recently, Lippmann and colleagues have developed a better mimetic model by demonstrating the derivation of brain endothelial cells from human induced pluripotent stem cells.⁵¹ In these studies, various methods were used to evaluate the structural and functional properties of the BBB. This included immunolabeling of tight junction proteins, such as ZO-1, Occludin and Claudin-5, permeability measurements of various types and sizes of molecules through the BBB and measurements of TEER. The TEER values measured *in vivo* have been reported to be as high as 5900 $\Omega\cdot\text{cm}^2$ which is markedly larger than that achieved by the majority of the currently available *in vitro* models.⁴⁹ In order to replicate *in vivo* TEER values in BBB models, endothelial cells have been co-cultured with other brain cell types, exposed to physiological shear stress⁵² or treated with various chemicals.⁵³ The models using cell lines, such as hCMEC/D.3, in co-culture with astrocytes have yielded relatively low TEER values⁵⁴ of 140 $\Omega\cdot\text{cm}^2$, whereas TEER values as high as 300 $\Omega\cdot\text{cm}^2$ ⁵⁵ were achieved utilizing primary endothelial cells from rodents and has been extensively reviewed.⁵⁶ Lippmann et al. recently developed a co-culture model with iPSC-derived endothelial cells and neuronal progenitor cells in conjunction with chemical treatment to promote BBB formation.⁵³ In their model, they showed that retinoic acid treatment can increase the TEER values up to 4000 $\Omega\cdot\text{cm}^2$ and sustain it above 2000 $\Omega\cdot\text{cm}^2$ for four consecutive days. The majority of the studies focused on developing *in vitro* models using commercially available TEER equipment as previously described in this paper.

Several microfluidic platforms have been recently developed to improve BBB models by more precisely controlling biochemical and mechanical factors in the BBB microenvironment.⁵⁷ Due to design limitations and the small scale of microfluidic systems, it is not suitable to use conventional TEER electrodes. Instead, custom-built microelectrodes are usually integrated or inserted into the system without disrupting the culture conditions. A multi-layered microfluidic device comprising of four PDMS substrates, two glass layers, a porous polycarbonate membrane sandwiched between PDMS layers, and integrated thin-film electrodes has been reported.⁵⁷ The thin-film microelectrodes were fabricated by depositing layers of Cr, Au and Ag on glass, followed by chlorination of the silver surface chemically to generate an electrochemically active AgCl surface. For TEER measurements, these electrodes were connected to a commercial EVOM system that was described in a previous section. By exposing the cells to dynamic conditions which provide shear stress simulation, the TEER of b.End3 (endothelial) cells in co-culture with C8D1A cells (astrocytic) was increased to 250 $\Omega\cdot\text{cm}^2$. A PDMS based BBB microfluidic platform to perform mechanical and biochemical modulation¹⁴ of the BBB that is comprised of the

immortalized human brain endothelial cell line hCMEC/D3 has been developed. To perform TEER measurements,¹⁴ an impedance/gain phase analyzer was coupled with two Pt wires (200 μm diameter) that were inserted through the PDMS side walls of the device. An impedance spectrum was recorded by applying the AC signal over the Pt electrodes with an amplitude of 0.2V in a frequency range of 100 Hz to 10 MHz. TEER values were estimated by fitting the measured impedance spectrum to an equivalent electrical circuit by applying a least-square optimization method.

Microfluidic models of BBB in combination with TEER measurement validation are promising for drug testing studies. The incorporation of recent human iPSC-derived EC models into microfluidic BBB platforms with physiologically relevant TEER values provide more realistic models for these studies.

5. Gastrointestinal Tract Models

Drug administration orally is usually preferred as it reduces any infection or pain associated with other invasive routes, is patient-friendly and doesn't require administration by medical personnel. However, the transport of drugs via the intestinal membrane is a complex and dynamic process that includes the passage of compounds across several pathways in parallel.¹¹ The intestinal mucosa is characterized by the presence of villi that constitutes the anatomical and functional unit for nutrient and drug absorption. The mucosa consists of an epithelial layer, the lamina propria and the muscularis mucosa.¹¹ Figure 5 (adapted from Antonissen et al.⁵⁸) indicates a schematic of the various components of a gastrointestinal (GI) tract model. The epithelial layer is considered to be the limiting hurdle for GI tract drug permeation and is therefore the histological component of most interest for *in vitro* recapitulation. The bioavailability of nutrients or drugs administered orally depends on the quality of the barrier function of the GI tract and is an important determinant, especially when investigating passive transport of substances through tight junctions. Tight junction complexes restrict passive substance diffusion through the paracellular spaces between epithelial cells, a process that can be compromised in diseased epithelial tissue.⁵⁹⁻⁶⁰ Active transport mechanisms enable the transport of substances through the cell bodies of epithelial cells. Both active and passive transport can be better investigated when the barrier function of the GI tract tissue is established to mimic either healthy or disease conditions in the human body.

At present, there are numerous cell lines and their co-cultures being studied for *in vitro* models of the GI tract. The most widely used cell line for developing human GI tract *in vitro* models is the Caco-2 line, derived from a human colorectal adenocarcinoma. These cells can be maintained easily in cell culture for many weeks and are capable of establishing tight junctions in culture. After 2-3 weeks, Caco-2 cells form a densely populated cell layer differentiating spontaneously into polarized enterocytes and a monolayer of columnar cells that are coupled together by tight junction protein complexes.⁶¹⁻⁶² The Caco-2 monolayer generates a TEER of 150-400 $\Omega\cdot\text{cm}^2$ that restricts the diffusion of substances across the barrier. Caco-2 cells are often used for studying nutrient and drug transport as they provide the main routes of substance transport from: 1) the paracellular route through tight junction

complexes, 2) the passive transcellular route through the bodies of epithelial cells, 3) the active, carrier-mediated paracellular through cells, and 4) transcytosis.⁶³

Caco-2 cells alone do not fully represent the morphology and physiology of GI tract. The GI tract consists of a number of other cell types, particularly goblet cells that do not form tight junctions. Goblet cells are mucus-producing cells that coat the epithelium with a layer of mucus, providing an additional diffusion barrier that plays a role in nutrient uptake.⁶⁴ Peyer patches are formed from aggregated lymphoid cells, allow passage of large peptides and also do not form tight junctions; Peyer patches constitute less than 0.5% of the human intestine. Although other cell types (e.g. paneth and enteroendocrine cells) are present in much smaller numbers,⁶⁵ few groups have begun to include even cells such as goblet cells and lymphocytes into their *in vitro* models.⁶⁶⁻⁶⁷ By including these cells, the strength of barrier function of such models is altered, rendering them more permeable and physiological.

A careful characterization of transport properties and TEER measurements will help in developing physiological models when utilizing immortalized cells lines. For example, immortalized cell lines such as HT29-MTX cells (goblet-type) have the potential to overgrow compared to Caco-2 cells when introduced into the culture in high numbers, giving rise to different barrier properties. To prevent this alteration in barrier properties, initial seeding ratios can be adjusted and the culture's relevance to physiologic transport can be tested.⁶⁸ In addition, selecting cultures with similar (or a minimum) TEER value before experimentation can be useful in preventing large variations in determination of transport rates due to unintended overgrowth.

IEC-18 cells, a small intestinal crypt-derived rat cell line, have been studied mainly for screening passive transcellular and paracellular transport of hydrophilic molecules.⁶⁹ Also, IEC-18 cells can simulate properties of the small intestine and could also simulate a leakiness/tightness of the paracellular pathway similar to human intestinal tissue.⁶⁹ However, IEC-18 cells are less well differentiated than the Caco-2 cells and not much is known about the carrier-mediated transport systems in these cell lines. TC-7 cells,⁷⁰ which are a subclone of Caco-2 cells, have also been studied for permeability screening and display higher enzyme content when compared with native Caco-2 cells. A co-culture model based on Caco-2 cells and human Raji B lymphocytes which are known to convert enterocytes into M cells (microfold cells) has been developed. The Caco-2/Raji B co-culture model has been applied to study the absorption of large molecules and nanoparticles containing drugs.⁷¹

Human primary GI tract cells harvested from patient samples mimic nutrient and drug transport with the highest similarity to *in vivo* conditions. These samples can contain all the different cell types of the GI tract to enable the re-establishment of 3D organization *in vitro* when appropriate 3D scaffolds are provided.⁷² Wang et al. have tested this approach with murine GI tract cells, finding that the cells generated continuous millimeter-scale tissue that resembled the architecture and geometry of the colonic epithelium *in vivo*.

Depending on the study to be conducted, researchers may choose to use different cells types or cell lines to model nutrient and drug transport, keeping in mind that the cell types used in the *in vitro* model as well as the cell culture conditions will determine the TEER that will be

observed. Table 2 shows a range of some of the TEER values reported for GI tract models. Yee et al. discussed the problem of comparing TEER data across laboratories, suggesting that determining the permeability coefficients for substances may provide a more accurate basis for cross-laboratory comparison.⁷³ In addition, including other cell types into the model, such as mucus-producing goblet cells, has the potential to decrease TEER values which may make the model more physiological. GI epithelia are classified⁷⁴ based on TEER values as “tight” indicated by values of about 2000 $\Omega\cdot\text{cm}^2$, as “intermediate” indicated by values in the range of 300-400 $\Omega\cdot\text{cm}^2$ and as “leaky” indicated by values of 50-100 $\Omega\cdot\text{cm}^2$.

After the inception of microfluidic organs-on-chips, several groups have developed microfluidic models of the GI tract where apical and basolateral sides are accessible via microfluidic streams.^{68, 75-81} Some of these groups have already begun to utilize multiple cell types to develop GI tract models and combine them with models of liver tissue to investigate inter-organ relationships.^{68, 76, 80} The barrier function in microfluidic GI tract models has alternatively been evaluated by determining the permeability coefficients for fluorescently labeled dextran or standard drugs for which coefficients in intact cell cultures are known.⁷⁷

However those microfabricated systems that are designed for TEER measurements can offer TEER data in addition to permeability coefficients.⁷⁸ With the system developed by Kim et al., TEER values of up to 3000 to 4000 $\Omega\cdot\text{cm}^2$ were observed in the microfluidic system, while control cultures that were cultured under static conditions exhibited TEER values between 700 to 800 $\Omega\cdot\text{cm}^2$. The authors have not discussed whether the TEER values obtained from the static and microfluidic system are directly comparable. Nevertheless, such systems may make it possible to investigate the influence shear stress has on the barrier function of *in vitro* GI tract tissues. Also, these very high values of TEER are certainly not physiologic,⁷⁴ reducing the value of the system to replicate human physiology.

6. Pulmonary Models

The surface of the lung is lined with a continuous epithelium that can be divided into airway and alveolar epithelia. Figures 6 (adapted from Hollenhorst, 2011⁸² shows a schematic of the various cells of the airway and alveolar epithelium respectively. The gold standard culturing technique for obtaining physiologically relevant and functional pulmonary epithelium is to culture cells to confluence in liquid covered condition (LCC) followed by culture at an air-liquid interface (ALI).⁸³ Pulmonary epithelial cells secrete surfactants, develop tight junctions and differentiate into a specific cell type⁸³ when cultured at ALI for longer times. Many conventional and microfluidic *in vitro* pulmonary models representing pulmonary physiology have been developed by applying this culture technique that are comprised of primary cells, cell-lines and co-culture models.⁸⁴ The recent advances in microfabrication techniques have led to the development of microfluidic platforms for pulmonary models to incorporate and recapitulate complex physiological functions *in vitro*.⁸⁵⁻⁸⁶

6.1 Airway Epithelial Models

The airway epithelium is comprised of ciliated, clara, goblet and undifferentiated basal cells that are expressed in different proportions in nasal, tracheal and bronchial conducting airways.⁸² Airway epithelium can be damaged due to shear stress or mechanical ventilation and dysfunction of surfactant production. Patients with asthma and chronic obstructive pulmonary disease (COPD) have varying levels of inflammation and remodeling in these airways. A study of *in vitro* airway models to mimic airway epithelia can greatly enhance the understanding of small airway injury. Primary airway epithelial cell cultures have been isolated from several species including rat, hamster, guinea pig, dog, rabbit, bovine, horse and human.⁸⁴

The human tracheal epithelia and bronchial epithelia obtained from healthy donors first cultured at an ALI indicated TEER values of 700 - 1200 $\Omega\cdot\text{cm}^2$,⁸³ and closely matched the transcriptional profile of *in vivo* epithelia, thereby indicating the importance of culturing at an ALI.⁸³ These cultures differentiated to represent *in vivo* morphological and physiological properties that enabled the study of epithelial signaling pathways and Table 3 shows a range of values reported for pulmonary models.

Primary normal human bronchial epithelial (NHBE) cells have been developed and characterized for studying drug transport. A monolayer of NHBE cells sub-cultured up to passage 3 in an ALI on Transwell membrane inserts indicated a peak TEER value of $766\pm 154 \Omega\cdot\text{cm}^2$ 7 days after seeding.⁸⁷ It was observed that NHBE cultures on collagen-and fibronectin-coated Transwell membrane inserts treated with low levels of all-trans-retinoic acid showed remarkably higher TEER values between days 5 and 7, to over 1500 $\Omega\cdot\text{cm}^2$, and plateaued at 3000 $\Omega\cdot\text{cm}^2$ after 14 days.⁸⁸ It was concluded that the long-term NHBE cell cultures on modified surfaces could have formed better tight junctions that resulted in higher TEER values. A commercial system utilizing a human tracheobronchial cell monolayer exhibiting differentiated ciliated and goblet cells has been developed to study drug transport across barriers.⁸⁹ Another *in vitro* model using Human Nasal Epithelial (HNE) cells cultured in serum-free media has been developed and maximum TEER values of 3133 ± 665 , 2703 ± 407 and $1235\pm 74 \Omega\cdot\text{cm}^2$ for passages 2, 3 and 4 respectively have been reported. The TEER value dropped suddenly to around 500 $\Omega\cdot\text{cm}^2$ after day-2 and remained steady for 10 days.⁹⁰ An *in vitro* disease model of asthma has been developed based on primary human bronchial epithelial cells from bronchial brushings of asthma patients which were grown and differentiated at an ALI for 21 days. Confocal microscopy of normal differentiated cultures had continuous tight junction protein staining, whereas cultures of asthma patients had altered protein localization and discontinuous tight junction formation which resulted in lower TEER values.⁹¹ However, primary cells are not only difficult to obtain but also are complicated with respect to establishing a stable and reproducible culture.

Cell lines provide an alternative to primary cells. Human airway epithelial cell lines, such as Calu-3 and 16HBE14o,⁹² are widely used since they form polarized monolayers with tight junctions. A wide range of TEER values have been reported for Calu-3 cells varying from as low as 100 $\Omega\cdot\text{cm}^2$,⁹³ to as high as 2500 $\Omega\cdot\text{cm}^2$.⁹⁴ A TEER value of $1126\pm 222 \Omega\cdot\text{cm}^2$ has been reported⁹⁵ for Calu-3 monolayers on a transwell insert when measured with STX2/

EVOM. In contrast, much lower TEER values of 300-600 $\Omega\cdot\text{cm}^2$,⁹⁶ when measured with STX2/EVOM, have also been reported for Calu-3 monolayers on Transwell inserts. These differences in TEER values reported for the Calu-3 monolayers on filters when measured with STX2/EVOM could be due to differences in measurement techniques, growth conditions that strongly influence the differentiation process, cell morphology and tight junction formation.⁹⁵ TEER of Calu-3 cells cultured in microwells (50 - 60 $\Omega\cdot\text{cm}^2$) and measured using STX-3/EVOM electrodes have been reported to be six times lower than Calu-3 on Transwell inserts⁹⁷ when measured using STX2/EVOM. Similar to Calu-3, several new cell lines, such as NuLi-1, have been developed and have been observed to have a peak TEER value of $685\pm 31 \Omega\cdot\text{cm}^2$ at passage 1 which decreased to $389\pm 21 \Omega\cdot\text{cm}^2$ after 30 passages.⁹⁸ Cell lines mimicking the altered conditions found for diseases such as Cystic Fibrosis (CF) have also been developed to compensate for the limited availability of the actual diseased tissue. Some of the widely used CF airway epithelial cell line mimics include NCF3, CFT1, CFBE41o-, CuFi-3 and CuFi-4.⁸⁴ Ehrhardt et al., have studied CFBE41o- cells and measured the TEER in both LCC and ALI culture conditions separately. CFBE41o- cells cultured under an ALI developed a TEER below 250 $\Omega\cdot\text{cm}^2$ after 16 days, possibly due to less than optimal formation of cell-cell contact which is representative of the conditions in CF patients.⁹² However, when cultured under LCC conditions, the TEER values of CFBE41o- cells increased and a peak value of $1,156\pm 75 \Omega\cdot\text{cm}^2$ was reached after 16 days.

It is important to achieve geometric, kinematic and dynamic similarity between the *in vitro* and *in vivo* lung environment. The complex physiology of the small airways in lungs makes it currently impossible to recapitulate *in vitro*.⁹⁹ Microfluidic models may mimic the *in vivo* airway architecture and hence recreate mechanical flexibility and physiological levels of pulmonary pressures, which enables the investigation of treatments for airway reopening. The first microfluidic device to investigate the injuries caused by movement of liquid plugs in finite lengths was developed by seeding primary human small airway epithelial cells (SAEC) in a three dimensional cell culture with an ALI. The device was validated by analyzing the cell perfusate by ELISA for CC10, a marker for Clara cell differentiation. By modulating the air pressure and liquid volumetric flows, a propagation velocity of 3 to 5 mm/s to match the expected velocities in the terminal airways was achieved.⁹⁹ A more stable and functional small airway microfluidic model was developed using human alveolar epithelial (A549) cells cultured on Transwell inserts with an ALI.¹⁰⁰ The barrier properties at both the interfaces were determined by measuring TEER values using a MilliCell-ERS system (Millipore AG) over the course of 6 days. TEER values continuously increased and reached a maximum of 128 $\Omega\cdot\text{cm}^2$ and 152 $\Omega\cdot\text{cm}^2$ on the liquid and air interfaces respectively.¹⁰⁰ The model also revealed that liquid plugs caused significant injury to airway epithelia with a lower quantity or absence of surfactant. However, the extent of injury may vary depending on the cell type used since primary airway epithelial cells form much tighter junctions than cell lines and are more resistant to mechanical forces (shear, pressure and gradients), thereby preserving the epithelium integrity.¹⁰⁰ A more complex 3D *in vitro* model of physiologically relevant human upper airways was developed using Calu-3 epithelial cells, MRC-5 fibroblasts and dendritic cells grown on scaffolds. The model indicated a peak TEER value of 200 $\Omega\cdot\text{cm}^2$ which is similar to *in vivo* TEER of rabbit

airway epithelium ($260 - 320 \Omega \cdot \text{cm}^2$) when measured using EVOM and STX2 chopstick electrodes.¹⁰¹ A developed and validated *in vitro* model of airways would allow monitoring of cellular signaling of airway epithelia to elucidate potential mechanisms of small airway disorders.

6.2 Alveolar Epithelial Models

Alveoli are considered to be the functional unit of a lung. The alveolar epithelium lines the wall of the alveolus by the creating an ALI that facilitates an exchange of gases and is estimated to cover an average surface area of $100\text{-}140 \text{ m}^2$ in humans.¹⁰² The alveolar epithelium is made up of two epithelial cell types, namely, the terminally differentiated squamous alveolar epithelial type-I (AT-I) and the surfactant-producing cuboidal alveolar epithelial type-II (AT-II) cells.¹⁰²

The first conventional alveolar epithelium model based on primary rat alveolar type II cells (RAEpC) were cultured on polycarbonate membrane inserts and a TEER value of greater than $2000 \Omega \cdot \text{cm}^2$ was measured after 5 days.¹⁰³ Adson et al. were able to reproduce RAEpC monolayers capable of producing higher TEER values two days after seeding but the TEER values dropped to approximately $300 \Omega \cdot \text{cm}^2$ after 5 days.¹⁰⁴ Dickinson et al. cultured the most reproducible tight monolayers showing a TEER value of $2320 \pm 511 \Omega \cdot \text{cm}^2$ 3 days after seeding¹⁰⁵ and the TEER value remained relatively constant, decreasing slowly until day 8 to $1570 \pm 61 \Omega \cdot \text{cm}^2$. Fuchs et, al developed an *in vitro* model using human AT-II epithelial cells (HAEpC) seeded on collagen/fibronectin-coated Transwell inserts with the monolayer reaching confluence after 6-8 days¹⁰⁶ and with a TEER value of $1000\text{-}2000 \Omega \cdot \text{cm}^2$. Conventional alveolar models are difficult to culture and lose their ability to maintain tight junctions over a period of time

Apart from the primary cells, several cell lines such as A549, R3/1 and L-2, MLE-12, MLE-15, NCI-H441 and NCI-TT1 of alveolar origin have been used to develop *in vitro* models.⁸⁴ Of these, the human alveolar epithelial cell line (A549) is widely studied as it closely represents the morphological and biochemical characteristics of human pulmonary cells. However, they lack the ability to form tight junctions leading to lower TEER values of $45 \Omega \cdot \text{cm}^2$ that reached a peak value of $100 \Omega \cdot \text{cm}^2$ after dexamethasone treatment.¹⁰⁷ In order to obtain better tight junctions and recapitulate the alveolar epithelial barrier, a co-culture of human pulmonary microvascular endothelial cells (HPMEC) were used in conjugation with NCI-H441 or A549 cells to study the pathogenesis and recovery during acute lung injury. Co-cultures of NCI-H441 and HPMEC produced significantly higher TEER value of $565 \pm 48 \Omega \cdot \text{cm}^2$ after treatment with dexamethasone.¹⁰⁸ Similarly, another co-culture model utilizing HPMECs with isolated primary human type-II alveolar epithelial cells (HAT-II) was developed by culturing cells on both sides of the permeable membrane to form a bilayer. This model enables the study of pathomechanisms and toxicological studies at the alveolar-capillary barrier.¹⁰⁹ Although these models form a barrier, they do not incorporate other cell types such as macrophages and mast cells to study the inflammatory responses upon exposure to hazardous materials. An advanced 3D model of the alveolar epithelial barrier consisting of four cell lines was developed to study aerosol exposure to new nano-scale hazardous materials.¹¹⁰ This 3D model comprised A549 cells, differentiated

macrophage-like cells (THP-1), mast cells (HMC-1) and endothelial cells (EA.hy 929) cultured on a microporous membrane. The mast cells and macrophages were present on top of the A549 cells and did not enhance the tight junction formation, thereby causing lower TEER values ($250 \Omega \cdot \text{cm}^2$). This co-culture with 4 cell lines under an ALI secreted only 50% of Interleukin-8 (IL-8) and reacted more efficiently to reactive oxygen species (ROS) stimulation¹¹⁰ when compared to an LCC culture. This 3D system displayed a morphological resemblance to the *in vivo* organization of an alveolar capillary barrier but did not however have the required complexity to measure mechanical properties such as stress.

Many stable and viable microfluidic *in vitro* epithelial models have been developed comprised of A549 cells cultured under an ALI with TEER values ranging from 120 - 195 $\Omega \cdot \text{cm}^2$.^{111,112} These microfluidic implementations were observed to have better viability, monolayer integrity and surfactant production. To create an alveolar-capillary (epithelial) barrier, a triple co-culture model using hAEPc or A549 epithelial cells with macrophages and dendritic cells was developed. This triple co-culture model was observed to mimic a more realistic cellular barrier to test the effects of inhaled toxins and xenobiotics, but generated lower TEER values compared to individual epithelial cultures.¹¹³ The mechanical strain induced inflammatory response as well as the toxic effects of nanoparticles have been studied by developing a biomimetic microfluidic system comprising human alveolar epithelial cells and pulmonary microvascular endothelial cells on opposing sides of a porous PDMS membrane, with a peak TEER value of $> 800 \Omega \cdot \text{cm}^2$. The system functionality was demonstrated by incorporating bacteria and neutrophils. The system was also used to recapitulate whole organ responses to mimic alveolar epithelium exposed to ultrafine silica particles under mechanical stress which caused increased intracellular ROS levels.⁸⁵ To date, none of the microfluidic systems built to measure pulmonary function have electrodes embedded to obtain real-time TEER measurements. An *in vitro* model representing the complex morphology and physiological functions of a lung would be an invaluable drug discovery tool.

7. Other *in vitro* barrier models

Apart from the barrier models described in the previous sections, there are other *in vitro* barrier models that have been developed for predicting drug transport. These include placental,¹¹⁴ nasal,¹¹⁵ vaginal,¹¹⁶ ocular¹¹⁷ and skin¹¹⁸ based *in vitro* models. The focus of this paper was restricted to BBB, GI tract and pulmonary models, since they are more widely studied than the other models and so comparisons could be made between different methods and techniques.

8. Factors affecting TEER measurements

8.1 Temperature

TEER measurements have been shown^{3, 119} to be temperature dependent. Ideally, TEER measurements should be conducted in an incubator at 37°C which requires that the electrical measurement setup have access to or be placed within the incubator. Otherwise, if TEER measurements are performed at room temperature, it would be necessary to first equilibrate

temperature before performing TEER measurements to avoid any temperature fluctuation induced TEER changes, however this could be detrimental to cell physiology and function. Typically, equilibration from 37°C to room temperatures requires at least 20 minutes. To overcome these problems and to allow TEER measurements during cooling or heating, a mathematical method has been developed¹²⁰ to correct TEER values for the actual temperature at which they were recorded and is referred to as temperature-corrected TEER (tcTEER). To calculate tcTEER values it is required to record temperature accurately during the experiment. The calculation of tcTEER would permit comparison of TEER values measured at various temperatures across independent experiments and perhaps even between different laboratories.¹²⁰ The application of tcTEER not only eliminates the need of performing temperature equilibration when experiments are performed outside an incubator, but also saves time and minimizes the temperature fluctuations that the cells are exposed to that could be detrimental to their function.

8.2 Cell passage number

The effect of passage number of Caco-2 cells on TEER measurements has been studied. TEER values were compared¹²¹ between the early passages of Caco-2 cells (Caco-2E, passages 35-47) and later passages of the cells (Caco-2L, passages 87-112). It was observed that the TEERs for Caco-2E cells ranged from 475 – 700 $\Omega\cdot\text{cm}^2$ when compared to Caco-2L cells which ranged from 1100 – 1500 $\Omega\cdot\text{cm}^2$. Transmission electron microscopy studies of these two cell populations revealed¹²¹ that regions of Caco-2L cells were composed of multiple cells layers rather than the monolayers observed in Caco-2E cells even though the epithelial cell height (barrier thickness) was not significantly different. Also, intercellular and intracellular lumina were observed in the Caco-2L cells, but not in Caco-2E cells. It was concluded¹²¹ that while intracellular lumina may not influence TEER values, the multiple cell layers and intercellular lamina may have significant impact on TEER measurements by changing the tightness and/or the length of the paracellular pathway. Another study¹²² on the effect of passage number on TEER values has also been reported where Caco-2 cells from passage 20 through passage 109 were examined. It was observed that TEER values increased until passage 36, then the resistance was variable until passage 70, after which there was a decline in TEER value until passage 100.

8.3 Cell culture medium composition

The origin of cell lines and the different protocols used to maintain these cells in culture can vary between laboratories and can affect the process of spontaneous differentiation that leads to a phenotype expressing many morphological and functional characteristics of mature cells. For example, in the case of Caco-2 cells, the degree of differentiation achieved with serum free- and serum reduced media has been studied³² to verify the establishment of the intestinal barrier by TEER measurements. It was observed that differentiation in a commercial mixture MITO+™ serum extender (Becton Dickinson, Bedford, MA, USA) resulted in cell monolayers with significantly lower TEER values when compared to the control cells in an FBS symmetric medium (complete DMEM supplemented with 10% FBS on both apical and basolateral sides). The lower TEER value was attributed³² to changes in molecular organization of the tight junctions and/or activated ionic channels caused by treatment with MITO+™. However, lower TEER values were not considered a

disadvantage, since physiological TEER values are lower¹²³ than Caco-2 cells differentiated in FBS containing medium. It was concluded that the lower TEER values of the Caco-2 cells differentiated in MITO+™ may better represent *in vivo* permeability than Caco-2 cells cultured in serum containing or ITS media.

8.4 Cell culture period

Another variable of importance when utilizing the Caco-2 cell line or other endothelial lines, that can cause variation in experimental conditions is the optimum time after seeding to provide a uniform differentiated culture for experimentation. The culture period is considered to be important for the formation of a tight junction in these cells.¹²⁴ The conventional culture period of Caco-2 cells for transport studies is considered to be 21 days. However, these cells have been reported to be used for nutrient transport studies as early as 6-9 days after seeding,¹²⁵ 18-21 days after seeding,¹²² or others have found 30 days after seeding to be optimal.¹²⁶ The influence of the culture period on the transcellular transport activity and expression levels of efflux transporters such as human multidrug resistance 1 (hMDR1), human multidrug resistance-associated protein 2 (hMRP2), and human breast cancer resistance protein (hBCRP) in Caco-2 cells has been investigated.¹²⁷ These transporters are known to have an important role in drug bioavailability as they contribute to drug efflux and drug-drug interactions. Caco-2 cells were cultured for a period of up to 6 weeks and it was observed that the TEER value at 3 weeks was the highest.¹²⁷ However, after 2-weeks in culture, the transcellular transport activities of hMDR1, hMRP2, and hBCRP were observed to be high enough to perform transport studies to identify whether a compound is a substrate for hMDR1, hMRP2, and hBCRP.

TEER-related mechanoelectronicsThe most widely used and commercially available TEER measurement system is the EVOM and includes a pair of electrodes known as a STX2/“chopstick” electrode pair. The position of the STX2 electrodes can introduce variability between measurements if the positioning is not consistent. The introduction of STX2 electrodes into the well under test requires careful handling to prevent any disturbance to the cells under study. This problem can be overcome by development of integrated microelectrodes within these systems. The positioning of integrated microelectrodes in close proximity to the cellular layer can also reduce contribution of electrical resistance from cell culture medium and also minimize the signal noise generated by electrode motion. The uniformity of the current density generated by the measurement electrodes is also known to affect the TEER values. The diameter of the permeable membrane must be compatible with the geometry of the electrodes to achieve uniform current density. In custom made microfluidic implementations, the symmetry of the electrode geometry on both sides of the membrane can help achieve uniform current densities. To verify the uniformity of current density an electrical simulation/modeling study should be performed in cases where non-conventional electrode designs are incorporated into a TEER measurement system. In custom designed electrical measurement equipment/set up for impedance spectroscopy based TEER measurements, it is important to isolate the effects of parasitic capacitance¹²⁸ by parameter extraction using theoretical analyses and equivalent circuit simulations.

8.5 Shear Stress

Shear stress has a mechanotransductive effect on several endothelial molecular pathways through activation of membrane bound receptors.¹²⁹ These pathways stimulate increased gene and protein expression leading to production of tight junction proteins such as ZO-1,¹³⁰ and modulate cytoskeletal structure promoting cell reorientation and restructuring.¹³¹ Shear stress can affect the barrier functions of endothelial cells and therefore TEER values of endothelial cells, under flow conditions which can be different from that of static culture. The effect of laminar fluid shear stress on the permeability of endothelial cells and the resulting TEER values has been studied based on impedance spectroscopy investigation of confluent cultures of porcine pulmonary trunk endothelial cells.¹³² It was observed that the TEER value of the endothelial cells ranged between 6 and 15 $\Omega \cdot \text{cm}^2$ while under both resting conditions and low shear stress levels (0.5 dyne/cm²). Increasing the shear stress to the range of 2-50 dyne/cm² caused a transient 2-15% increase in TEER values within 15 minutes and was accompanied by a reduction in cell motility and acceleration of cell shape change. Subsequently, TEER values slowly decreased to a minimum of 20% below the starting value. TEER values eventually recovered to reach control levels within hours and a deceleration in shape change was also observed. A heterogeneous distribution of α -, β -, and γ -catenin, the main components of the endothelial adherens type junctions, was also observed, indicating a differentiated regulation of shear stress-induced junction rearrangement.¹³²

9. TEER Measurement – Significance and current challenges

TEER values are accepted as strong indicators of the integrity of the cellular barriers before they are evaluated for transport of drugs or chemicals. Impedance spectroscopy, in combination with equivalent circuit analysis, provides a more accurate representation of TEER values than the DC/single frequency AC measurement approach. The use of cells cultured under static conditions on permeable membranes of standard cell culture inserts with external STX2 electrodes is predominant. In order for these studies to be physiologically relevant, it is necessary to develop *in vitro* systems that can mimic *in vivo* conditions. Recently many microfluidic platforms have been developed to more precisely control biochemical and mechanical factors in the cellular microenvironment. Microfluidic platforms can allow the exposure of cells to dynamic conditions which provide shear stress simulation wherever applicable. The integration of microelectrodes within these systems would allow continuous monitoring of cells without disrupting the cell structure. However, there are electrical and microfluidic packaging challenges that would have to be overcome for these microfluidic platforms to be more widely used in labs for long term drug transport studies. TEER measurements can be a good benchmark for barrier integrity when comparing results from different sources if the results of these measurements are correlated with the numerous factors that affect the TEER values. The design of *in vitro* models should allow reproduction of TEER values close to *in vivo* conditions since the success of these models for drug development depends on how closely they mimic the complexity of drug absorption of the *in vivo* barriers.

10. Conclusions

TEER measurement is a valuable non-invasive technique that can be applied to quantify the barrier integrity of cells during their various stages of growth and differentiation. Organs-on-chips or body-on-a-chip systems integrated with TEER measurement capability can be an excellent high-throughput and cost-effective tool for drug toxicity and permeability predictions during the early stages of drug discovery. Numerous *in vitro* cell models composed of immortalized cells that can be grown on semipermeable supports under controlled conditions have been studied for drug permeability and absorption evaluation. The success of these studies to predict drug absorption depends on how closely the *in vitro* models can mimic the complexity of the drug absorption processes of the *in vivo* barriers. TEER measurements based on impedance spectroscopy are more reliable and provide more information about the cells when compared to the Ohm's law method. Even though TEER measurement systems are commercially available, integration of a TEER measurement system within the chip-based devices allows continuous non-invasive monitoring of the cells within an incubator without disrupting the cell culture environment. TEER measurements for various cell types have been reported with commercially available measurement setups and also with custom built microfluidic implementations. Also, for the same cell type, a wide range of TEER values have been reported in the literature. These variations can arise due to various factors affecting values such as the accuracy of the measurement techniques based on selection and usage of electrodes, temperature during measurement, medium formulation, cell culture period and passage number of cells used in the model. It may not always be possible to control every variable, but the aim should be to optimize and simplify conditions whenever needed. TEER values have proven to be simple and rapid indicators of cellular barrier integrity. However, in order to make a meaningful comparison of TEER results reported from different laboratories, it is important to not merely compare the values but also take into consideration all the above factors that affect TEER. Also, when reporting TEER values, laboratories should identify and report the above listed variables and the exact conditions under which TEER measurements were performed. The goal of *in vitro* models with respect to TEER measurement should be to reproduce the TEER values observed under *in vivo* conditions. Any use of models with TEER values much higher/lower than *in vivo* values may lead to incorrect conclusions while evaluating transport of drugs or chemicals.

Acknowledgments

The authors would like to acknowledge funding support from the National Institutes of Health, NCATS Microphysiological Systems grant number UH2TR000516.

References

1. Ryan, US. Endothelial Cells. Taylor & Francis; 1988.
2. Schwab, M. Encyclopedia of cancer. 3rd. Springer; Heidelberg; New York: 2011.
3. Matter K, Balda MS. Functional Analysis of Tight Junctions. Methods. 2003; 30:228–234. [PubMed: 12798137]
4. Huh D, Kim HJ, Fraser JP, et al. Microfabrication of Human Organs-on-Chips. Nat Protoc. 2013; 8:2135–2157. [PubMed: 24113786]

5. Ariza-Nieto M, Prot JM, Shuler ML. Human Body-on-a-Chip: A Tool to Study Health Disorders That Involve Modulations of the “Methylation Pathway”. *In Vitro Cell Dev Biol Anim.* 2012; 48:49–50.
6. Esch MB, Mahler GJ, Stokol T, et al. Body-on-a-Chip Simulation with Gastrointestinal Tract and Liver Tissues Suggests that Ingested Nanoparticles Have the Potential to Cause Liver Injury. *Lab Chip.* 2014; 14:3081–3092. [PubMed: 24970651]
7. Esch MB, Smith AST, Prot JM, et al. How Multi-Organ Microdevices can Help Foster Drug Development. *Adv Drug Deliv Rev.* 2014; 69:158–169. [PubMed: 24412641]
8. Sung JH, Esch MB, Prot JM, et al. Microfabricated Mammalian Organ Systems and Their Integration into Models of Whole Animals and Humans. *Lab Chip.* 2013; 13:1201–1212. [PubMed: 23388858]
9. Sung JH, Srinivasan B, Esch MB, et al. Using Physiologically-Based Pharmacokinetic-Guided “Body-on-a-Chip” Systems to Predict Mammalian Response to Drug and Chemical Exposure. *Exp Biol Med (Maywood, NJ).* 2014
10. Zucco F, Batto AF, Bises G, et al. An Inter-Laboratory Study to Evaluate the Effects of Medium Composition on the Differentiation and Barrier Function of Caco-2 Cell Lines. *Atla- Altern Lab Anim.* 2005; 33:603–618. [PubMed: 16372835]
11. Sarmento B, Andrade F, Silva SBd, et al. Cell-Based in Vitro Models for Predicting Drug Permeability. *Expert Opin Drug Metab Toxicol.* 2012; 8:607–621. [PubMed: 22424145]
12. Balimane PV, Chong S, Morrison RA. Current Methodologies Used for Evaluation of Intestinal Permeability and Absorption. *J Pharmacol Toxicol Methods.* 2000; 44:301–12. [PubMed: 11274897]
13. Esch M, Sung J, Yang J, et al. On Chip Porous Polymer Membranes for Integration of Gastrointestinal Tract Epithelium with Microfluidic ‘Body-on-a-Chip’ Devices. *Biomed Microdevices.* 2012; 14:895–906. [PubMed: 22847474]
14. Griep LM, Wolbers F, de Wagenaar B, et al. BBB on Chip: Microfluidic Platform to Mechanically and Biochemically Modulate Blood-Brain Barrier Function. *Biomed Microdevices.* 2013; 15:145–50. [PubMed: 22955726]
15. Franke H, Galla HJ, Beuckmann CT. An Improved Low-Permeability in Vitro-Model of the Blood–Brain Barrier: Transport Studies on Retinoids, Sucrose, Haloperidol, Caffeine and Mannitol. *Brain Res.* 1999; 818:65–71. [PubMed: 9914438]
16. Muruganandam A, Herx LM, Monette R, et al. Development of Immortalized Human Cerebromicrovascular Endothelial Cell Line as an in Vitro Model of the Human Blood-Brain Barrier. *FASEB J.* 1997; 11:1187–97. [PubMed: 9367354]
17. Bowman PD, Ennis SR, Rarey KE, et al. Brain Microvessel Endothelial-Cells in Tissue-Culture - A Model for Study of Blood-Brain-Barrier Permeability. *Ann Neurol.* 1983; 14:396–402. [PubMed: 6638956]
18. Plateel M, Dehouck MP, Torpier G, et al. Hypoxia Increases the Susceptibility to Oxidant Stress and the Permeability of the Blood-Brain-Barrier Endothelial-Cell Monolayer. *J Neurochem.* 1995; 65:2138–2145. [PubMed: 7595500]
19. Deli MA, Dehouck MP, Cecchelli R, et al. Histamine Induces a Selective Albumin Permeation Through the Blood-Brain Barrier in Vitro. *Inflamm Res.* 1995; 44 Suppl 1:S56–7. [PubMed: 8521001]
20. Plateel M, Teissier E, Cecchelli R. Hypoxia Dramatically Increases the Nonspecific Transport of Blood-Borne Proteins to the Brain. *J Neurochem.* 1997; 68:874–877. [PubMed: 9003080]
21. Annunziata P, Cioni C, Toneatto S, et al. HIV-1 gp120 Increases the Permeability of Rat Brain Endothelium Cultures by a Mechanism Involving Substance P. *Aids.* 1998; 12:2377–2385. [PubMed: 9875575]
22. Horibe Y, Hosoya Ki, Kim KJ, et al. Polar Solute Transport Across the Pigmented Rabbit Conjunctiva: Size Dependence and the Influence of 8-Bromo Cyclic Adenosine Monophosphate. *Pharm Res.* 1997; 14:1246–1251. [PubMed: 9327456]
23. Duffy SL, Murphy JT. Colorimetric Assay to Quantify Macromolecule Diffusion Across Endothelial Monolayers. *BioTechniques.* 2001; 31:495–6. 498, 500–1. [PubMed: 11570492]

24. Audus K, Borchardt R. Characterization of an in Vitro Blood–Brain Barrier Model System for Studying Drug Transport and Metabolism. *Pharm Res.* 1986; 3:81–87. [PubMed: 24271465]
25. Dehouck MP, Méresse S, Dehouck B, et al. In Vitro Reconstituted Blood-Brain Barrier. *J Control Release.* 1992; 21:81–91.
26. Benson K, Cramer S, Galla HJ. Impedance-Based Cell Monitoring: Barrier Properties and Beyond. *Fluids Barriers CNS.* 2013; 10:5. [PubMed: 23305242]
27. Epithelial VoltOhmmeter. <http://www.wpi-europe.com/products/cell-and-tissue/teer-measurement/evom2.aspx>
28. Haorah J, Schall K, Ramirez SH, et al. Activation of Protein Tyrosine Kinases and Matrix Metalloproteinases Causes Blood-Brain Barrier Injury: Novel Mechanism for Neurodegeneration Associated with Alcohol Abuse. *Glia.* 2008; 56:78–88. [PubMed: 17943953]
29. Watson PMD, Paterson JC, Thom G, et al. Modelling the Endothelial Blood-CNS Barriers: A Method for the Production of Robust in Vitro Models of the Rat Blood-Brain Barrier and Blood-Spinal Cord Barrier. *BMC Neurosci.* 2013; 14
30. EndOhm Chamber. <http://www.wpi-europe.com/products/cell-and-tissue/teer-measurement/endohm-24snap.aspx>
31. Bernas MJ, Cardoso FL, Daley SK, et al. Establishment of Primary Cultures of Human Brain Microvascular Endothelial Cells to Provide an in Vitro Cellular Model of the Blood-Brain Barrier. *Nat Protoc.* 2010; 5:1265–1272. [PubMed: 20595955]
32. Ferruzza S, Rossi C, Sambuy Y, et al. Serum-Reduced and Serum-Free Media for Differentiation of Caco-2 Cells. *ALTEX.* 2013; 30:159–168. [PubMed: 23665805]
33. Li H, Sheppard DN, Hug MJ. Transepithelial Electrical Measurements with the Ussing Chamber. *J Cyst Fibros.* 2004; 3 Suppl 2:123–6. [PubMed: 15463943]
34. Douville NJ, Tung YC, Li R, et al. Fabrication of Two-Layered Channel System with Embedded Electrodes to Measure Resistance Across Epithelial and Endothelial Barriers. *Anal Chem.* 2010; 82:2505–2511. [PubMed: 20178370]
35. Macdonald, JR.; Johnson, WB. *Impedance Spectroscopy.* John Wiley & Sons, Inc.; 2005. *Fundamentals of Impedance Spectroscopy*; p. 1-26.
36. Jovov B, Wills NK, Lewis SA. A Spectroscopic Method for Assessing Confluence of Epithelial-Cell Cultures. *Am J Physiol.* 1991; 261:C1196–C1203. [PubMed: 1767820]
37. Duan Y, Gotoh N, Yan QS, et al. Shear-Induced Reorganization of Renal Proximal Tubule Cell Actin Cytoskeleton and Apical Junctional Complexes. *Proc Natl Acad Sci USA.* 2008; 105:11418–11423. [PubMed: 18685100]
38. Walker GM, Zeringue HC, Beebe DJ. Microenvironment Design Considerations for Cellular Scale Studies. *Lab Chip.* 2004; 4:91–97. [PubMed: 15052346]
39. Atencia J, Beebe DJ. Controlled Microfluidic Interfaces. *Nature.* 2005; 437:648–655. [PubMed: 16193039]
40. Ayliffe HE, Frazier AB, Rabbitt RD. Electric Impedance Spectroscopy Using Microchannels with Integrated Metal Electrodes. *J Microelectromech Syst.* 1999; 8:50–57.
41. Wilhelm I, Fazakas C, Krizbai IA. In Vitro Models of the Blood-Brain Barrier. *Acta Neurobiol Exp (Wars).* 2011; 71:113–128. [PubMed: 21499332]
42. Wong A, Ye M, Levy A, et al. The Blood-Brain Barrier: An Engineering Perspective. *Front Neuroeng.* 2013; 6
43. Prabhakarandian B, Shen MC, Nichols JB, et al. SyM-BBB: A Microfluidic Blood Brain Barrier Model. *Lab Chi.* 2013; 13:1093–1101.
44. Hawkins RA, O’Kane RL, Simpson IA, et al. Structure of the Blood-Brain Barrier and its Role in the Transport of Amino Acids. *J Nutr.* 2006; 136:218S–226S. [PubMed: 16365086]
45. Neuhaus W, Lauer R, Oelzant S, et al. A Novel Flow Based Hollow-Fiber Blood-Brain Barrier in Vitro Model with Immortalised Cell Line PBMEC/C1-2. *J Biotechnol.* 2006; 125:127–141. [PubMed: 16730091]
46. Sobue K, Yamamoto N, Yoneda K, et al. Induction of Blood-Brain Barrier Properties in Immortalized Bovine Brain Endothelial Cells by Astrocytic Factors. *Neurosci Res.* 1999; 35:155–164. [PubMed: 10616919]

47. Deli MA, Abraham CS, Kataoka Y, et al. Permeability studies on in vitro blood-brain barrier models: Physiology, pathology, and pharmacology. *Cell Mol Neurobiol.* 2005; 25:59–127. [PubMed: 15962509]
48. Crone C, Christensen O. Electrical Resistance of a Capillary Endothelium. *J Gen Physiol.* 1981; 77:349–71. [PubMed: 7241087]
49. Butt AM, Jones HC, Abbott NJ. Electrical-Resistance Across the Blood-Brain-Barrier in Anesthetized Rats - A Developmental-Study. *J Physiol (Lond).* 1990; 429:47–62. [PubMed: 2277354]
50. Crone C, Olesen SP. Electrical Resistance of Brain Microvascular Endothelium. *Brain Res.* 1982; 241:49–55. [PubMed: 6980688]
51. Lippmann ES, Azarin SM, Kay JE, et al. Derivation of Blood-Brain Barrier Endothelial Cells from Human Pluripotent Stem Cells. *Nat Biotechnol.* 2012; 30:783–91. [PubMed: 22729031]
52. Cucullo L, Hossain M, Puvenna V, et al. The Role of Shear Stress in Blood-Brain Barrier Endothelial Physiology. *BMC Neurosci.* 2011; 12:40. [PubMed: 21569296]
53. Lippmann ES, Al-Ahmad A, Azarin SM, et al. A Retinoic Acid-Enhanced, Multicellular Human Blood-Brain Barrier Model Derived from Stem Cell Sources. *Sci Rep.* 2014; 4:4160. [PubMed: 24561821]
54. Daniels BP, Cruz-Orengo L, Pasiaka TJ, et al. Immortalized Human Cerebral Microvascular Endothelial Cells Maintain the Properties of Primary Cells in an in Vitro Model of Immune Migration Across the Blood Brain Barrier. *J Neurosci Methods.* 2013; 212:173–9. [PubMed: 23068604]
55. Abbott NJ, Dolman DE, Drndarski S, et al. An Improved in Vitro Blood-Brain Barrier Model: Rat Brain Endothelial Cells Co-Cultured with Astrocytes. *Methods Mol Biol.* 2012; 814:415–30. [PubMed: 22144323]
56. Wilhelm I, Krizbai IA. In Vitro Models of the Blood-Brain Barrier for the Study of Drug Delivery to the Brain. *Mol Pharm.* 2014
57. Booth R, Kim H. Characterization of a Microfluidic in Vitro Model of the Blood-Brain Barrier (muBBB). *Lab Chip.* 2012; 12:1784–92. [PubMed: 22422217]
58. Antonissen G, Martel A, Pasmans F, et al. The Impact of Fusarium Mycotoxins on Human and Animal Host Susceptibility to Infectious Diseases. *Toxins.* 2014; 6:430–452. [PubMed: 24476707]
59. Powell D. Barrier function of epithelia. *Am J Physiol.* 1981; 241:G275–88. [PubMed: 7032321]
60. Kraehenbuhl JP, Pringault E, Neutra MR. Review article: Intestinal epithelia and barrier functions. *Aliment Pharmacol Ther.* 2010; 11:3–9. [PubMed: 9467973]
61. Ferruzza S, Rossi C, Scarino ML, et al. A Protocol for in Situ Enzyme Assays to Assess the Differentiation of Human Intestinal Caco-2 Cells. *Toxicol In Vitro.* 2012; 26:1247–1251. [PubMed: 22123491]
62. Matsumoto H, Erickson RH, Gum JR, et al. Biosynthesis of Alkaline Phosphatase During Differentiation of the Human Colon Cancer Cell Line Caco-2. *Gastroenterology.* 1990; 98:1199–1207. [PubMed: 2323513]
63. Artursson P, Palm K, Luthman K. Caco-2 Monolayers in Experimental and Theoretical Predictions of Drug Transport. *Adv Drug Deliv Rev.* 2001; 46:27–43. [PubMed: 11259831]
64. D EA. Nutrition and the Gut Mucosal Barrier. *Curr Opin Gen Surg.* 1993:85–91. [PubMed: 7584019]
65. Quaroni A, Hochman J. Development of Intestinal Cell Culture Models for Drug Transport and Metabolism Studies. *Adv Drug Deliv Rev.* 1996; 22:3–52.
66. Antunes F, Andrade F, Araújo F, et al. Establishment of a Triple Co-Culture in Vitro Cell Models to Study Intestinal Absorption of Peptide Drugs. *Eur J Pharm Biopharm.* 2012; 83:427–35. [PubMed: 23159710]
67. Mahler GJ, Shuler ML, Glahn RP. Characterization of Caco-2 and HT29-MTX Cocultures in an in Vitro Digestion/Cell Culture Model Used to Predict Iron Bioavailability. *The J Nutr Biochem.* 2009; 20:494–502. [PubMed: 18715773]
68. Mahler GJ, Esch MB, Glahn RP, et al. Characterization of a Gastrointestinal Tract Microscale Cell Culture Analog Used to Predict Drug Toxicity. *Biotechnol Bioeng.* 2009; 104:193–205. [PubMed: 19418562]

69. Steensma A, Noteborn H, Kuiper HA. Comparison of Caco-2, IEC-18 and HCEC Cell Lines as a Model for Intestinal Absorption of Genistein, Daidzein and Their Glycosides. *Environ Toxicol Pharmacol.* 2004; 16:131–139. [PubMed: 21782699]
70. Gres MC, Julian B, Bourrie M, et al. Correlation Between Oral Drug Absorption in Humans, and Apparent Drug Permeability in TC-7 Cells, a Human Epithelial Intestinal Cell Line: Comparison with the Parental Caco-2 Cell Line. *Pharm Res.* 1998; 15:726–733. [PubMed: 9619781]
71. des Rieux A, Fievez V, Theate I, et al. An Improved in Vitro Model of Human Intestinal Follicle-Associated Epithelium to Study Nanoparticle Transport by M Cells. *Pharm Acta Helv.* 2007; 30:380–391.
72. Wang Y, Ahmad AA, Sims CE, et al. In Vitro Generation of Colonic Epithelium from Primary Cells Guided by Microstructures. *Lab Chip.* 2014; 14:1622–1631. [PubMed: 24647645]
73. Yee S. In Vitro Permeability Across Caco-2 Cells (Colonic) Can Predict in Vivo (Small Intestinal) Absorption in Man—Fact or Myth - Springer. *Pharm Res.* 1997; 14:763–766. [PubMed: 9210194]
74. David, F. *Transport Processes in Pharmaceutical Systems.* Informa Healthcare; 1999. *Biological Transport Phenomena in the Gastrointestinal Tract.*
75. Brand R, Hannah T, Mueller C, et al. A Novel System to Study the Impact of Epithelial Barriers on Cellular Metabolism. *Ann Biomed Eng.* 2000
76. Choi S, Fukuda O, Sakoda A, et al. Enhanced Cytochrome P450 Capacities of Caco-2 and Hep G2 Cells in New Coculture System Under the Static and Perfused Conditions: Evidence for Possible Organ-to-Organ Interactions Against Exogenous Stimuli. *Mater Sci Eng C Mater Biol Appl.* 2004; 24:333–339.
77. Imura Y, Asano Y, Sato K, et al. A Microfluidic System to Evaluate Intestinal Absorption. *Anal Sci.* 2009; 25:1403–1407. [PubMed: 20009325]
78. Kim HJ, Huh D, Hamilton G, et al. Human Gut-on-a-Chip Inhabited by Microbial Flora that Experiences Intestinal Peristalsis-Like Motions and Flow. *Lab Chip.* 2012; 12:2165–2174. [PubMed: 22434367]
79. Kimura H, Yamamoto T, Sakai H, et al. An Integrated Microfluidic System for Long-Term Perfusion Culture and on-Line Monitoring of Intestinal Tissue Models. *Lab Chip.* 2008; 8:741. [PubMed: 18432344]
80. van Midwoud PM, Merema MT, Verpoorte E, et al. A Microfluidic Approach for in Vitro Assessment of Interorgan Interactions in Drug Metabolism Using Intestinal and Liver Slices. *Lab Chip.* 2010; 10:2778–2786. [PubMed: 20835427]
81. Yeon JH, Park JK. Drug Permeability Assay Using Microhole-Trapped Cells in a Microfluidic Device. *Anal Chem.* 2009; 81:1944–1951. [PubMed: 19203200]
82. Hollenhorst MI, Richter K, Fronius M. Ion Transport by Pulmonary Epithelia. *J Biomed Biotechnol.* 2011; 2011:16.
83. Pezzulo AA, Starnes TD, Scheetz TE, et al. The Air-Liquid Interface and Use of Primary Cell Cultures Are Important to Recapitulate the Transcriptional Profile of in Vivo Airway Epithelia. *Am J Physiol-Lung C.* 2011; 300:L25–L31.
84. Buckley, S.; Kim, KJ.; Ehrhardt, C. In Vitro Cell Culture Models for Evaluating Controlled Release Pulmonary Drug Delivery. In: Smyth, HDC.; Hickey, AJ., editors. *Controlled Pulmonary Drug Delivery.* Springer; New York: 2011. p. 417–442.
85. Huh D, Matthews BD, Mammoto A, et al. Reconstituting Organ-Level Lung Functions on a Chip. *Science.* 2010; 328:1662–1668. [PubMed: 20576885]
86. Long C, Finch C, Esch M, et al. Design Optimization of Liquid-Phase Flow Patterns for Microfabricated Lung on a Chip. *Ann Biomed Eng.* 2012; 40:1255–1267. [PubMed: 22271245]
87. Lin HX, Li H, Cho HJ, et al. Air-Liquid Interface (ALI) Culture of Human Bronchial Epithelial Cell Monolayers as an in Vitro Model for Airway Drug Transport Studies. *J Pharm Sci.* 2007; 96:341–350. [PubMed: 17080426]
88. Oshima T, Gedda K, Koseki J, et al. Establishment of Esophageal-Like Non-Keratinized Stratified Epithelium Using Normal Human Bronchial Epithelial Cells. *Am J Physiol-Cell Ph.* 2011; 300:C1422–C1429.

89. Hayden P. Application of Organotypic in Vitro Human Cell Culture Models for Research and Development of Inhalation Pharmaceutical Formulations Targeting the Proximal Airways. *Inhalation*. Oct.2012 2012.
90. Yoo JW, Kim YS, Lee SH, et al. Serially passaged Human Nasal Epithelial Cell Monolayer for in Vitro Drug Transport Studies. *Pharm Res*. 2003; 20:1690–6. [PubMed: 14620527]
91. Xiao C, Puddicombe SM, Field S, et al. Defective Epithelial Barrier Function in Asthma. *J Allergy Clin Immun*. 2011; 128:549–U177. [PubMed: 21752437]
92. Ehrhardt C, Collnot EM, Baldes C, et al. Towards an in Vitro Model of Cystic Fibrosis Small Airway Epithelium: Characterisation of the Human Bronchial Epithelial Cell Line CFBE41o. *Cell Tissue Res*. 2006; 323:405–415. [PubMed: 16249874]
93. Finkbeiner WE, Carrier SD, Teresi CE. Reverse Transcription-Polymerase Chain-Reaction (Rt-Pcr) Phenotypic Analysis of Cell-Cultures of Human Tracheal Epithelium, Tracheobronchial Glands, and Lung Carcinomas. *Am J Resp Cell Mol*. 1993; 9:547–556.
94. Lomans BP, Smolders A, Intven LM, et al. Formation of Dimethyl Sulfide and Methanethiol in Anoxic Freshwater Sediments. *Appl Environ Microbiol*. 1997; 63:4741–7. [PubMed: 16535751]
95. Mathia NR, Timoszyk J, Stetsko PI, et al. Permeability Characteristics of Calu-3 Human Bronchial Epithelial Cells: In Vitro-in Vivo Correlation to Predict Lung Absorption in Rats. *J Drug Target*. 2002; 10:31–40. [PubMed: 11996084]
96. Foster KA, Avery ML, Yazdanian M, et al. Characterization of the Calu-3 Cell Line as a Tool to Screen Pulmonary Drug Delivery. *Int J Pharm*. 2000; 208:1–11. [PubMed: 11064206]
97. Bol L, Galas JC, Hillaireau H, et al. A Microdevice for Parallelized Pulmonary Permeability Studies. *Biomed Microdevices*. 2014; 16:277–85. [PubMed: 24337430]
98. Zabner J, Karp P, Seiler M, et al. Development of Cystic Fibrosis and Noncystic Fibrosis Airway Cell Lines. *Am J Physiol-Lung C*. 2003; 284:L844–L854.
99. Huh D, Fujioka H, Tung YC, et al. Acoustically Detectable Cellular-Level Lung Injury Induced by Fluid Mechanical Stresses in Microfluidic Airway Systems. *Proc Natl Acad Sci USA*. 2007; 104:18886–91. [PubMed: 18006663]
100. Tavana H, Zamankhan P, Christensen PJ, et al. Epithelium Damage and Protection During Reopening of Occluded Airways in a Physiologic Microfluidic Pulmonary Airway Model. *Biomed Microdevices*. 2011; 13:731–742. [PubMed: 21487664]
101. Harrington H, Cato P, Salazar F, et al. Immunocompetent 3D Model of Human Upper Airway for Disease Modeling and In Vitro Drug Evaluation. *Mol Pharm*. 2014
102. Neuhaus W, Samwer F, Kunzmann S, et al. Lung Endothelial Cells Strengthen, but Brain Endothelial Cells Weaken Barrier Properties of a Human Alveolar Epithelium Cell Culture Model. *Differentiation*. 2012; 84:294–304. [PubMed: 23023065]
103. Kim KJ, Suh DJ. Asymmetric Effects of H₂O₂ on Alveolar Epithelial Barrier Properties. *Am J Physiol*. 1993; 264:L308–L315. [PubMed: 8460719]
104. Adson A, Raub TJ, Burton PS, et al. Quantitative Approaches to Delineate Paracellular Diffusion in Cultured Epithelial-Cell Monolayers. *J Pharm Sci*. 1994; 83:1529–1536. [PubMed: 7891269]
105. Dickinson PA, Evans JP, Farr SJ, et al. Putrescine Uptake by Alveolar Epithelial Cell Monolayers Exhibiting Differing Transepithelial Electrical Resistances. *J Pharm Sci*. 1996; 85:1112–6. [PubMed: 8897281]
106. Fuchs S, Hollins AJ, Laue M, et al. Differentiation of Human Alveolar Epithelial Cells in Primary Culture: Morphological Characterization and Synthesis of Caveolin-1 and Surfactant Protein-C. *Cell Tissue Res*. 2003; 311:31–45. [PubMed: 12483282]
107. Barar J. Modulation of Cellular Transport Characteristics of the Human Lung Alveolar Epithelia. *Iranian Journal of Pharmaceutical Research*. 2005; 3:163–171.
108. Hermanns MI, Unger RE, Kehe K, et al. Lung Epithelial Cell Lines in Coculture with Human Pulmonary Microvascular Endothelial Cells: Development of an Alveolo-Capillary Barrier in Vitro. *Lab Invest*. 2004; 84:736–52. [PubMed: 15077120]
109. Hermanns MI, Fuchs S, Bock M, et al. Primary Human Coculture Model of Alveolo-Capillary Unit to Study Mechanisms of Injury to Peripheral Lung. *Cell Tissue Res*. 2009; 336:91–105. [PubMed: 19238447]

110. Klein SG, Serchi T, Hoffmann L, et al. An Improved 3D Tetraculture System Mimicking the Cellular Organisation at the Alveolar Barrier to Study the Potential Toxic Effects of Particles on the Lung. *Part Fibre Toxicol.* 2013; 10
111. Nalayanda DD, Puleo C, Fulton WB, et al. An Open-Access Microfluidic Model for Lung-Specific Functional Studies at an Air-Liquid Interface. *Biomed Microdevices.* 2009; 11:1081–1089. [PubMed: 19484389]
112. Blank F, Rothen-Rutishauser BM, Schurch S, et al. An Optimized in Vitro Model of the Respiratory Tract Wall to Study Particle Cell Interactions. *J Aerosol Med.* 2006; 19:392–405. [PubMed: 17034314]
113. Lehmann AD, Daum N, Bur M, et al. An in Vitro Triple Cell Co-Culture Model with Primary Cells Mimicking the Human Alveolar Epithelial Barrier. *Eur J Pharm Biopharm e V.* 2011; 77:398–406.
114. Levkovitz R, Zaretsky U, Gordon Z, et al. In Vitro Simulation of Placental Transport: Part I. Biological Model of the Placental Barrier. *Placenta.* 2013; 34:699–707. [PubMed: 23764139]
115. Agu RU, Dang HV, Jorissen M, et al. Nasal Absorption Enhancement Strategies for Therapeutic Peptides: An in Vitro Study Using Cultured Human Nasal Epithelium. *Int J Pharm.* 2002; 237:179–191. [PubMed: 11955816]
116. Gorodeski GI. The Cultured Human Cervical Epithelium a New Model for Studying Paracellular Transport. *J Soc Gynecol Investig.* 1996; 3:267–280.
117. O'Sullivan NL, Baylor AE, Montgomery PC. Development of Immortalized Rat Conjunctival Epithelial Cell Lines: An in Vitro Model to Examine Transepithelial Antigen Delivery. *Exp Eye Res.* 2007; 84:323–331. [PubMed: 17123516]
118. Netzaff F, Lehr CM, Wertz PW, et al. The Human Epidermis Models EpiSkin (R), SkinEthic (R) and EpiDerm (R): An Evaluation of Morphology and Their Suitability for Testing Phototoxicity, Irritancy, Corrosivity, and Substance Transport. *Eur J Pharm Biopharm.* 2005; 60:167–178. [PubMed: 15913972]
119. Torres R, Pizarro L, Csendes A, et al. GTX 2/3 Epimers Permeate the Intestine Through a Paracellular Pathway. *J Toxicol Sci.* 2007; 32:241–8. [PubMed: 17785941]
120. Blume LF, Denker M, Gieseler F, et al. Temperature Corrected Transepithelial Electrical Resistance (TEER) Measurement to Quantify Rapid Changes in Paracellular Permeability. *Pharmazie.* 2010; 65:19–24. [PubMed: 20187574]
121. Lu S, Gough AW, Bobrowski WF, et al. Transport Properties Are Not Altered Across Caco-2 Cells with Heightened TEER Despite Underlying Physiological and Ultrastructural Changes. *J Pharm Sci.* 1996; 85:270–3. [PubMed: 8699327]
122. Briske Anderson MJ, Finley JW, Newman SM. The Influence of Culture Time and Passage Number on the Morphological and Physiological Development of Caco-2 cells. *Proc Soc Exp Biol Med.* 1997; 214:248–257. [PubMed: 9083258]
123. Le Ferrec E, Chesne C, Artusson P, et al. In Vitro Models of the Intestinal Barrier - The Report and Recommendations of ECVAM Workshop 46. *Altern Lab Anim.* 2001; 29:649–668. [PubMed: 11709041]
124. Sambuy Y, De Angelis I, Ranaldi G, et al. The Caco-2 Cell Line as a Model of the Intestinal Barrier: Influence of Cell and Culture-Related Factors on Caco-2 Cell Functional Characteristics. *Cell Biol Toxicol.* 2005; 21:1–26. [PubMed: 15868485]
125. Trotter PJ, Storch J. Fatty Acid Uptake and Metabolism in a Human Intestinal Cell Line (Caco-2): Comparison of Apical and Basolateral Incubation. *J Lipid Res.* 1991; 32:293–304. [PubMed: 2066664]
126. Thwaites DT, Hirst BH, Simmons NL. Substrate-Specificity of the Di/Tripeptide Transporter in Human Intestinal Epithelia (Caco-2)- Identification of Substrates that Undergo H⁺-Coupled Absorption. *Br J Pharmacol.* 1994; 113:1050–1056. [PubMed: 7858848]
127. Kamiyama E, Sugiyama D, Nakai D, et al. Culture Period-Dependent Change of Function and Expression of ATP-Binding Cassette Transporters in Caco-2 Cells. *Drug Metab Dispos.* 2009; 37:1956–1962. [PubMed: 19505989]
128. Zhang G, Zhu R. Effect of Parasitic Capacitance on Impedance Measurement and Model Extraction. *Electroanalysis.* 2010; 22:351–358.

129. Booth, RH.; Kim, H. In: Society, C. a. B. M., editor. A Parallel Array Microfluidic Blood-Brain Barrier Model for High-Throughput Quantitation of Shear Stress Effects; 16th International Conference on Miniaturized Systems for Chemistry and Life Sciences, MicroTAS 2012; Okinawa, Japan. Okinawa, Japan: 2012. p. 491-493.
130. Siddharthan V, Kim YV, Liu S, et al. Human Astrocytes/Astrocyte-Conditioned Medium and Shear Stress Enhance the Barrier Properties of Human Brain Microvascular Endothelial Cells. *Brain res.* 2007; 1147:39–50. [PubMed: 17368578]
131. Galbraith CG, Skalak R, Chien S. Shear Stress Induces Spatial Reorganization of the Endothelial Cell Cytoskeleton. *Cell Motil Cytoskeleton.* 1998; 40:317–30. [PubMed: 9712262]
132. Seebach J, Dieterich P, Luo F, et al. Endothelial Barrier Function Under Laminar Fluid Shear Stress. *Lab Invest.* 2000; 80:1819–31. [PubMed: 11140695]
133. Amin, R.; Artmann, T.; Artmann, G., et al. Permeability of an in Vitro Model of Blood Brain Barrier (BBB). In: Lim, C.; Goh, JH., editors. 13th International Conference on Biomedical Engineering. Vol. 23. Springer; Berlin Heidelberg: 2009. p. 81-84.
134. Balbuena P, Li W, Magnin-Bissel G, et al. Comparison of Two Blood-Brain Barrier in Vitro Systems: Cytotoxicity and Transfer Assessments of Malathion/Oxon and Lead Acetate. *Toxicol Sci.* 2010; 114:260–271. [PubMed: 20064834]
135. Nitz T, Eisenblatter T, Psathaki K, et al. Serum-derived Factors Weaken the Barrier Properties of Cultured Porcine Brain Capillary Endothelial Cells in Vitro. *Brain Res.* 2003; 981:30–40. [PubMed: 12885423]
136. Da Violante G, Zerrouk N, Richard I, et al. Short Term Caco-2/TC7 Cell Culture: Comparison Between of Conventional 21-D and a Commercially Available 3-D System. *Biol Pharm Bull.* 2004; 27:1986–1992. [PubMed: 15577218]
137. Hilgendorf C, Spahn-Langguth H, Regardh CG, et al. Caco-2 Versus Caco-2/HT29-MTX Co-Cultured Cell Lines: Permeabilities Via Diffusion, Inside- and Outside-Directed Carrier-Mediated Transport. *J Pharm Sci.* 2000; 89:63–75. [PubMed: 10664539]
138. Feighery LM, Cochrane SW, Quinn T, et al. Myosin Light Chain Kinase Inhibition: Correction of Increased Intestinal Epithelial Permeability in Vitro. *Pharm Res.* 2008; 25:1377–1386. [PubMed: 18163202]
139. Behrens I, Stenberg P, Artursson P, et al. Transport of Lipophilic Drug Molecules in a New Mucus-Secreting Cell Culture Model Based on HT29-MTX Cells. *Pharm Res.* 2001; 18:1138–1145. [PubMed: 11587485]
140. Cho MJ, Thompson DP, Cramer CT, et al. The Madin Darby Canine Kidney (MDCK) Epithelial-Cell Monolayer as a Model Cellular-Transport Barrier. *Pharm Res.* 1989; 6:71–77. [PubMed: 2470075]
141. Béduneau A, Tempesta C, Fimbel S, et al. A Tunable Caco-2/HT29-MTX Co-Culture Model Mimicking Variable Permeabilities of the Human Intestine Obtained by an Original Seeding Procedure. *Eur J Pharm Biopharm.* 2014; 87:290–298. [PubMed: 24704198]
142. Bazes A, Nollevaux G, Coco R, et al. Development of a Triculture Based System for Improved Benefit/Risk Assessment in Pharmacology and Human Food. *BMC Proc.* 2011; 5:67.
143. Bhat M, Toledovelasquez D, Wang L, et al. Regulation of Tight Junction Permeability by Calcium Mediators and Cell Cytoskeleton in Rabbit Tracheal Epithelium. *Pharm Res.* 1993; 10:991–997. [PubMed: 8378262]

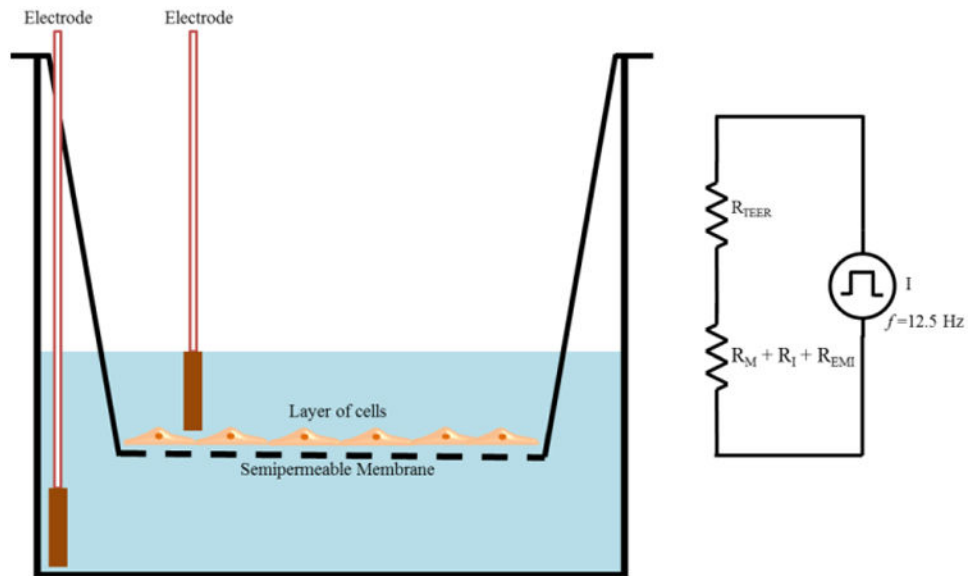


Figure 1. TEER measurement with chopstick electrodes. The total electrical resistance includes the ohmic resistance of the cell layer R_{TEER} , the cell culture medium R_M , the semipermeable membrane insert R_I and the electrode medium interface R_{EMI} .

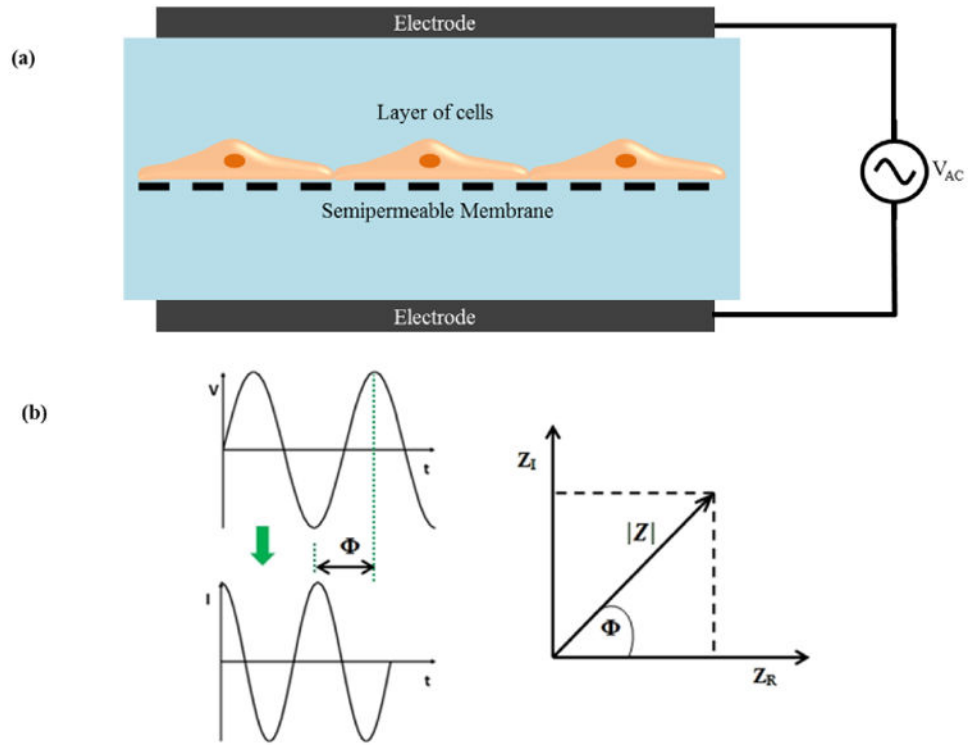


Figure 2. (a) TEER measurement concept based on impedance spectroscopy (b) Components of Impedance.

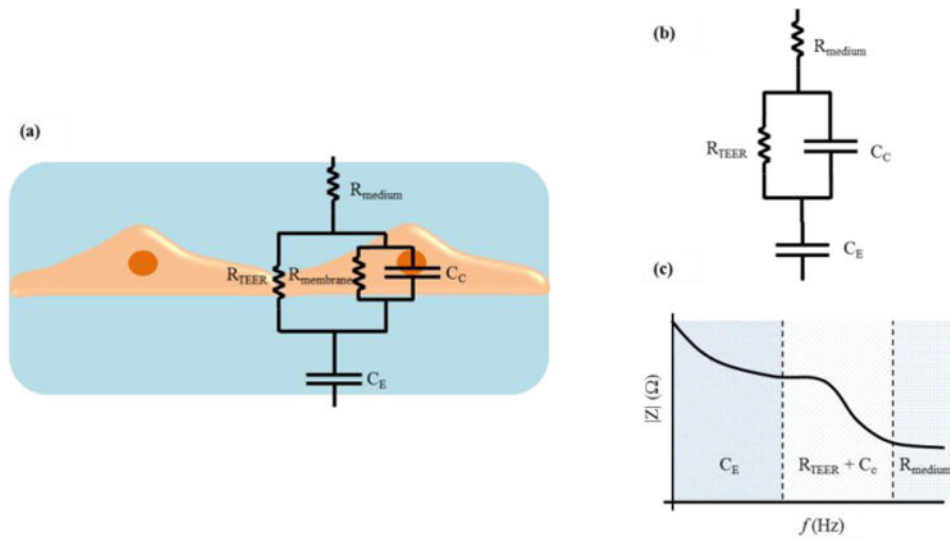


Figure 3. (a) A typical equivalent circuit diagram that can be applied to analyze the impedance spectrum of cellular systems. (b) Simplified equivalent circuit (c) A typical impedance spectrum with distinct frequency dependent regions. Adapted from Benson et al.²⁶

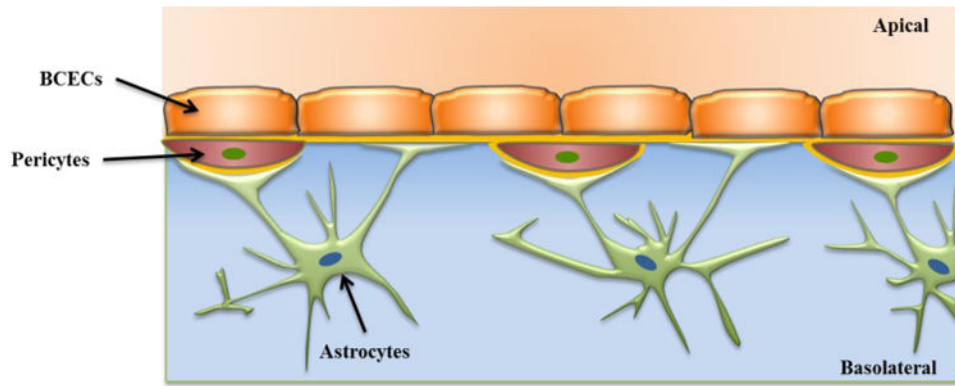


Figure 4. A schematic of BBB showing various components, brain capillary endothelial cells (BCECs), basement membrane, pericytes and astrocytes. Adapted from Wong et al.⁴²

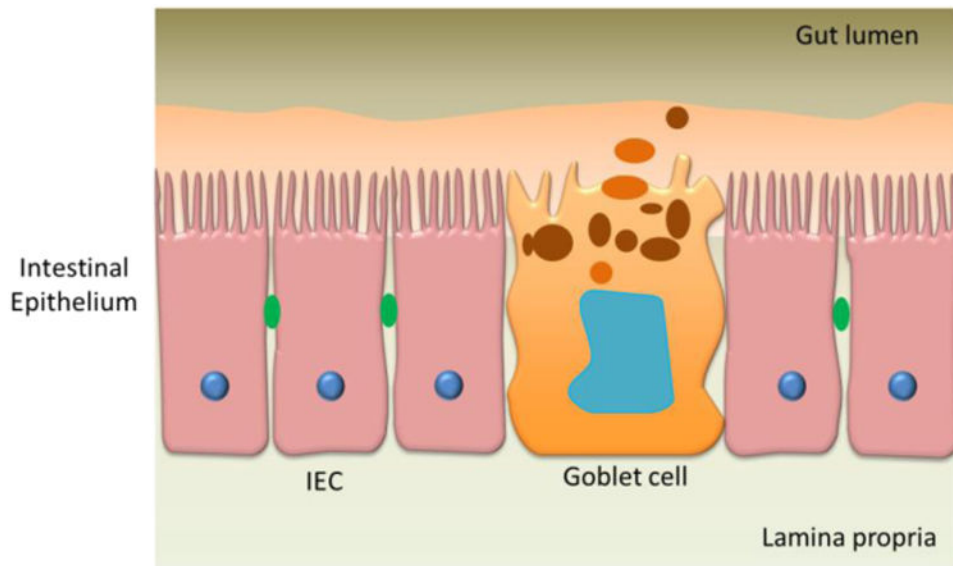


Figure 5. A schematic of the GI tract model showing various components, intestinal epithelial cells (IEC), goblet cell. Adapted from Antonissen et al.⁵⁹.

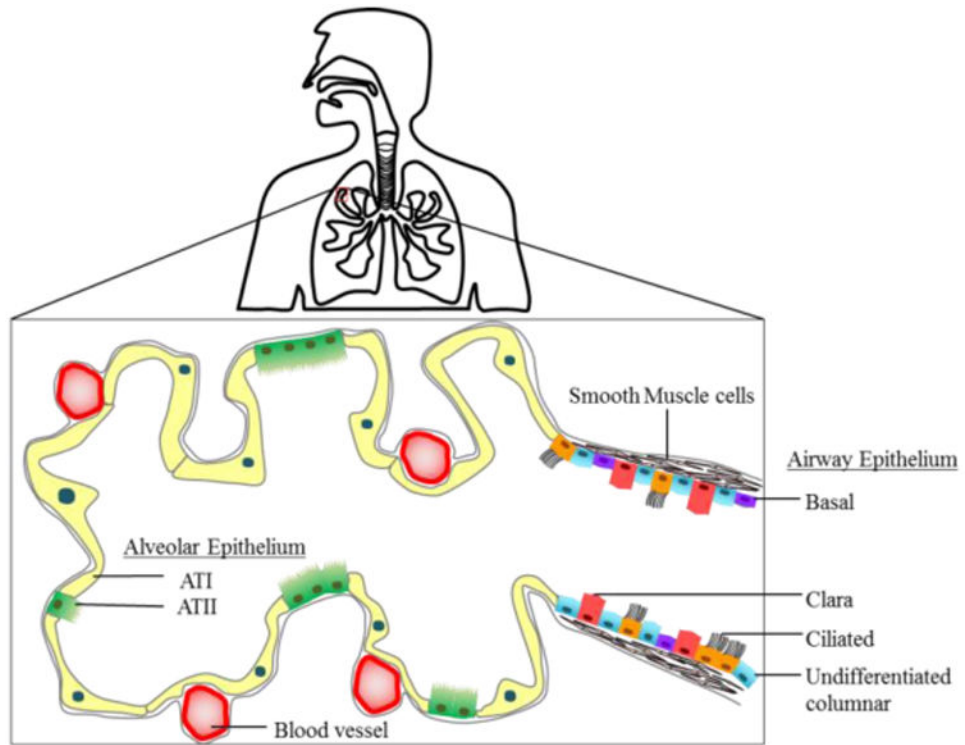


Figure 6.

A schematic overview of the human lung. Cells of the airway epithelium comprises ciliated, undifferentiated columnar, clara and basal cells. Cells of the alveolar epithelium comprise AT-I and AT-II type cells. Adapted from Hollenhorst, 2011.⁸²

Table 1
TEER values for BBB models

Cell type used in <i>In vitro</i> Model	TEER ($\Omega \cdot \text{cm}^2$)	Equipment Used	Ref
BBB (in vivo, rat)	5900	Two Microelectrodes/Cable theory	49
primary human brain microvascular endothelial cells (HBMEC's)	100	EVOM/Chopstick	54
Immortalized Human Brain Endothelial Cell Line (hCMEC/D3)	36.9 \pm 0.9	Impedance analyzer/Pt electrodes	14
hCMEC/D3	100	EVOM/Chopstick	54
hCMEC/D3 and primary human astrocytes	140	EVOM/Chopstick	54
Bovine Brain Microvascular Capillary Endothelial Cells (BBMCE) and Madin-Darby Canine Kidney (MDCK Epithelial Cells)	2020	EVOM/Endohm	133
Endothelial(RBE4) and rat astrocytes	490 - 510	Millicell-ERS/Endohm	134
Endothelial(BMCE) and rat astrocytes	250 - 300	Millicell-ERS/Endohm	134
b.End3 endothelial cells and C8-D1A astrocytes (microfluidic)	250	EVOM2/Custom electrodes	57
b.End3 endothelial cells and C8-D1A astrocytes (Transwell)	20	EVOM2/Endohm	57
Porcine brain microvessel endothelial cells	300 – 500 (serum)	EVOM/Endohm	15
	600 – 800 (serum free)		
Porcine brain microvessel endothelial cells	1200 - 1800	Impedance analyzer	135
Co-culture of Primary human brain pericytes, human astrocytes and neurons derived from human neural progenitor cells	4000	EVOM/STX-2	53

Table 2
TEER values for GI tract models

Cell type used in <i>In vitro</i> Model	TEER ($\Omega \cdot \text{cm}^2$)	Equipment Used	Ref
Gastric mucosa (in vivo)	2000	Ussing chambers	74
Colon (in vivo)	300-400	Ussing chambers	74
Small intestine (in vivo)	50 - 100	Ussing Chambers	74
human epithelial colorectal adenocarcinoma cells (Caco-2)	1100 - 1350	Millicell-ERS system	32
Caco-2/TC7	711 \pm 79	Millicell-ERS/Endohm	136
Rat small intestinal (IEC-18)	100	Millicell-ERS system	69
Human immortalized colon cell line (HCEC)	200	Millicell-ERS system	69
Caco-2	1400 - 2400	EVOM/Chopstick	137
Caco-2	763 \pm 287	EVOM/Endohm	138
Caco-2 and HT29-MTX	110 - 185	EVOM/Chopstick	137
HT29-MTX	25	EVOM/Endohm	139
MDCK	1500	Impedance analyzer/Ag electrodes	140
Caco - 2	250	Millicell-ERS system	141
Caco-2 amd HT29-MTX	122 \pm 19	Millicell-ERS system	142
Caco-2 amd HT29-MTX	100 - 300	Millicell-ERS system	141
Caco-2 and Raji B	285 \pm 76	Millicell-ERS/Endohm	71
Caco-2 and Raji B	88 \pm 27	Millicell-ERS system	142
Caco-2, HT29 and Raji B	60 \pm 17	Millicell-ERS system	142
Caco-2	3000 - 4000	Voltage-ohm meter/Ag electrodes	57

Table 3

TEER values for Pulmonary models.

Cell type used in <i>In vitro</i> Model		TEER ($\Omega \cdot \text{cm}^2$)	Equipment Used	Ref
Airway Epithelia	Rabbit airway epithelium (<i>in vivo</i>)	260 - 320	High-input impedance microvoltmeter/Ag/AgCl system	143
	Human Tracheal and Bronchial Epithelia (Donors)	700 - 1200	EVOM/STX2	83
	Primary Normal Human Bronchial Epithelial cells (NHBE)	766 \pm 154	EVOM	87
	Primary Normal Human Bronchial Epithelial cells (NHBE)	3000	Millicell-ERS/Chopstick	88
	Human Nasal Epithelial (HNE) cells	3133 \pm 665	EVOM/Endohm	90
	Human Bronchial Epithelial cell line (Calu-3)	300 - 600	EVOM/STX2	96
	Human Bronchial Epithelial cell line (Calu-3)	1126 \pm 222	EVOM/STX2	95
	Human Bronchial Epithelial cell line (Calu-3)	50 - 60 (in microwells)	EVOM/STX3	97
	Bronchial Epithelial cell line (NuLi-1)	685 \pm 31	Ussing Chambers Systems	98
	Human alveolar epithelial (A549) cell line	152	Millicell-ERS system	100
	Calu-3, MRC5 and dendritic cells	200	EVOM/STX2	101
	Diseased bronchial epithelial cell line(CFBE41o-)	250	EVOM/STX2	92
Alveolar Epithelia	Primary rat alveolar type II cells	2000	Ussing Chamber	103
	Primary rat alveolar type II cells	2320 \pm 511	EVOM	105
	Human Alveolar type-II Epithelial cells (HAEpC)	1000 - 2000	EVOM	106
	A549	45 - 100	EVOM/STX2	107
	A549	120 - 195	EVOM/Ag/AgCl	111
	A549	140	Millicell-ERS system	112
	Human pulmonary microvascular endothelial cells (HPMEC) and NCI-H441	565 \pm 48	EVOM/STX2	108
	Primary human type-II alveolar epithelial cells (HAT-II) and HPMEC	1730 \pm 460	EVOM/STX2	109
	A549, macrophage like cells(THP-1), mast cells(HMC-1), endothelial cells(EA.hy 929)	250	EVOM/STX2	54
	HAEpC, macrophages, dendritic cells	1113 \pm 30	Millicell-ERS system	113
Human alveolar epithelial and pulmonary microvascular endothelial cells	> 800	Volt-Ohm meter - Ag/AgCl electrodes	85	